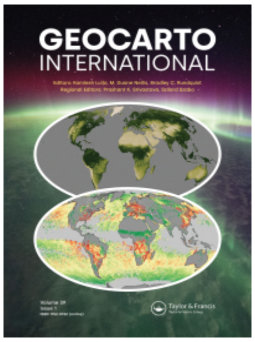

Geocarto International

ISSN: 1010-6049 (Print) 1752-0762 (Online) Journal homepage: www.tandfonline.com/journals/tgei20

Determining the sensitivity of Sentinel-2 bands to optically and non-optically active water quality parameters under high- and low-flow conditions in the cradle of Humankind World Heritage Site, South Africa

Sinesipho Ngamile , Mahlatse Kganyago , Sabelo Madonsela & Vuyelwa Mvandaba

To cite this article: Sinesipho Ngamile , Mahlatse Kganyago , Sabelo Madonsela & Vuyelwa Mvandaba (2026) Determining the sensitivity of Sentinel-2 bands to optically and non-optically active water quality parameters under high- and low-flow conditions in the cradle of Humankind World Heritage Site, South Africa, Geocarto International, 41:1, 2663616, DOI: 10.1080/10106049.2026.2663616

To link to this article: https://doi.org/10.1080/10106049.2026.2663616

Published online: 29 Apr 2026.

GEOCARTO INTERNATIONAL
2026, VOL. 41, NO. 1, 2663616
https://doi.org/10.1080/10106049.2026.2663616

RESEARCH ARTICLE

Determining the sensitivity of Sentinel-2 bands to optically and non-optically active water quality parameters under high- and low-flow conditions in the cradle of Humankind World Heritage Site, South Africa

Sinesipho Ngamile[a,b], Mahlatse Kganyago[a], Sabelo Madonsela[a,c] and Vuyelwa Mvandaba[d]

[a]Department of Geography, Environmental Management and Energy Studies, University of Johannesburg, Johannesburg, South Africa; [b]Research, Application, and Development Unit, Earth Observations Directorate, South African National Space Agency, Pretoria, South Africa; [c]Precision Agriculture Research Group, Advanced Agriculture and Food, Council for Scientific and Industrial Research (CSIR), Pretoria, South Africa; [d]Smart Water Resources Management, Water Centre, Council for Scientific and Industrial Research, Pretoria, South Africa

ABSTRACT

Access to clean water is a global challenge, particularly in the Global South, where scarcity and pollution threaten human and ecosystem health. Traditional water quality monitoring is limited in spatial and temporal coverage, while satellite remote sensing provides an alternative for assessing optically and non-optically active water quality parameters (WQPs). This study evaluated the sensitivity of Sentinel-2 MSI bands to WQPs in the Cradle of the Humankind World Heritage Site, South Africa, an area impacted by acid mine drainage. In situ measurements of DO, EC, pH, temperature, chlorophyll-a, and suspended solids were collected from 40 sites under high- and low-flow conditions. The Sentinel-2 images were atmospherically corrected, resampled to 10 m, and the values were extracted to the sampling points. Using multiple linear regression, random forest, and partial dependence plots methods, results showed that DO strongly influenced most bands, while suspended solids dominated the optically active band responses.

ARTICLE HISTORY
Received 23 January 2026
Accepted 17 April 2026

KEYWORDS
Water quality monitoring; water quality parameters; Sentinel-2 MSI; sensitivity analysis

1. Introduction

Access to clean water remains a global challenge, with 4 billion people lacking safe drinking water, particularly in the Global South, where 2.3 billion live in water-scarce regions, including 733 million in Asia, Africa, and Latin America (Biswas and Tortajada 2019; Hasan et al. 2023). Additionally, anthropogenic activities such as industrial waste disposal, urbanisation, and agricultural runoff further degrade water quality (Thakur and Devi 2024). Global initiatives such as the UN Sustainable Development Goal (SDG) 6 aim to address these issues by promoting access to clean water and sanitation (Hasan et al. 2023). In sub-Saharan Africa, where 90% of surface water is shared across borders, regional frameworks such as the Intergovernmental Science-Policy Platform for Water Sustainability are important for strengthening water security and policy coordination (Anghileri et al. 2024). Therefore, it is essential to apply these various global, regional and local policies, as water quality degradation continues to harm human and ecosystem health (Makanda et al. 2022). However, their effective implementation hinges on access to regular and accurate information about the water quality status of surface water resources. Currently, such information is lacking, especially in sub-Saharan Africa.

Water quality information is traditionally assessed by monitoring various biological, chemical, and physical parameters, such as chlorophyll-*a*, total suspended solids, dissolved oxygen (DO), pH, temperature, nitrogen (N), phosphorus (P), and turbidity, using in-situ sampling and laboratory analysis (Ahmed et al. 2020; Zainurin et al. 2022). However, despite being accurate, in situ and laboratory-based techniques for water quality assessment are labour-intensive, expensive, time-consuming and often limited in spatial

CONTACT Sinesipho Ngamile ngamilesinesipho20@gmail.com
Supplemental data for this article can be accessed online at https://doi.org/10.1080/10106049.2026.2663616.

and temporal coverage (Adjovu et al. 2023a; Sent et al. 2021). Earth observation satellites offer a cost-effective and scalable alternative. The satellite sensors capture spectral data across various wavelengths, making it possible to capture changes in the physical, chemical, and biological properties of water bodies (Bresciani et al. 2019). Studies (Ahmed et al. 2022; Gao et al. 2024; Sagan et al. 2020; Usali and Ismail 2010) have shown that such data can be used to monitor both optically active and non-optically active water quality parameters. For instance, the Moderate Resolution Imaging Spectroradiometer (MODIS), combined with machine learning, was used to track dissolved oxygen (DO) levels in Lake Taiu, China, from 2002 to 2021, showing a range of 7.2–14.2 mg/L, with a mean of 9.3 mg/L (Liu et al. 2022). However, while MODIS's high temporal resolution facilitates frequent water quality assessments, its low resolution limits its effectiveness for smaller inland water bodies (Li et al. 2022).

In contrast, new generation sensors, such as the Sentinel-2 multispectral instrument (MSI), offer high spatial and temporal resolutions, which are essential for assessing water quality in smaller inland water bodies. This advantage makes Sentinel-2 MSI an essential tool for regional water management (Soomets et al., 2020). For instance, Salas and Kumaran, 2022 used Sentinel-2 imagery at 10 m spatial resolution to map DO in Ohio's Little Miami River and identified B5 (Red-Edge) and B8 (near infrared) as key spectral predictors. These results demonstrate not only the spatial prowess of Sentinel-2 MSI but also the effectiveness of its spectral configuration, particularly the red-edge bands, in monitoring water quality parameters with high accuracy. Moreover, studies such as Liu et al. (2022) and Salas and Kumaran, 2022 have combined the use of satellite data with in situ data and machine learning to validate satellite data and improve their accuracy. For instance, Salas and Kumaran, 2022 used Sentinel-2 MSI and selected eight sampling sites along the Little Miami River for developing machine learning models (random forest and support vector machine) to predict DO in water bodies. The results revealed the red edge (B5) and near-infrared (B8) bands as key predictors of DO, with minimal errors (RMSE: 0.201–0.241 mg/L). Liu et al. (2022) used MODIS Aqua data and collected 847 data samples to develop an eXtreme gradient boosting (XGB) model for DO measurements in Lake Taihu. The results showed that water temperature, chlorophyll-*a*, and water clarity significantly influenced DO variability over two decades (RMSE: 1.28 mg/L). Both studies highlight the importance of integrating satellite data with field validation to increase the reliability of remote sensing and machine learning for water quality monitoring.

Despite the promising results achieved with Sentinel-2 MSI in previous studies (e.g. Salas and Kumaran, 2022), it remains unclear which spectral bands are most sensitive to specific water quality parameters. Sensitivity analysis – an approach that assesses how the uncertainty of an output (dependent variable) is influenced by its input (independent variable) (Saltelli and Puy 2021) – can help clarify these relationships. Understanding the relationships between spectral reflectance and water quality parameters is essential for developing robust models and improving the accuracy and reliability of spatiotemporal assessments of both optically and non-optically active water quality parameters. In most cases, only a few input variables have a major impact on the output, while the remaining variables have little or no effect (Razavi et al. 2021). Sensitivity analysis techniques identify such important variables using either the global sensitivity analysis (GSA) or local sensitivity analysis (LSA) methods. The LSA assesses how a single input parameter affects a model's output while keeping the other input parameters fixed. In contrast, the GSA methods, such as derivative-based, distribution-based, variogram-based and regression-based approaches, assess the entire range of input parameters by analysing how the changes in the input parameters contribute to the overall and corresponding changes in the output parameters (Razavi and Gupta 2015).

In the context of understanding the spectral response to variations in multiple interacting water quality parameters, LSA is limited by its focus on only one parameter at a time and ignores the inherent interactions between parameters (Díaz et al. 2023). As Zhang et al. (2015) attest, the GSA methods provide the advantage of handling complex systems with a range of inputs where they can effectively interact and provide results about parameter interactions and nonlinear or complex input behaviours. This, in turn, improves model accuracy and reliability. Furthermore, the GSA methods enhance our understanding of how model inputs influence outputs to assist in identifying important variables and their interactions (Zhang et al. 2015). Typically, relationships between input and output variables are established using linear regression. For instance, a study by Loaiza et al. (2023a, 2023b) assessed the effectiveness of Landsat-8 data in accurately estimating total organic carbon, total dissolved solids, and chlorophyll-*a* in the Humaya River basin of Mexico. The study used a linear regression model to correlate the Landsat-8 spectral reflectance with the water quality parameters. Afterwards, the model was refined by removing spectral bands that did not have a significant relationship with the parameters, showing the sensitivity of the Landsat-8 bands to the parameters and improving the accuracy of the results (i.e. R^2 of 0.926 for total organic carbon, R^2 of 0.88 for total dissolved solids and R^2 of 0.810 for chlorophyll-*a*).

However, linear regression is limited to linear relationships only and may not work for non-linear or complex relationships (Razavi et al. 2021). Consequently, the introduction of machine learning regression algorithms such as random forest (RF) are widely used for assessing complex relationships between input variables and outputs (Razavi et al. 2021). Mpakairi et al. (2024) developed and used a random forest model with Landsat-8 and Sentinel-2 data to assess the concentration of chlorophyll-*a* in South Africa's Nandoni Reservoir and found that Sentinel-2 MSI red-edge bands were most effective in achieving this task. Additionally, there are various ways in which the random forest model (and other models) visualizes the relationship between an input and output (i.e. response variable), as Random Forest has used Gini importance to explain this relationship. Other studies, however, have used post hoc model-agnostics such as partial dependence plots (PDPs), which determine the impact of a single variable while holding others constant, enhancing the understanding of each parameter's contribution to the predictive model (Johnson et al. 2022). For example, DeLuca et al. (2018) used partial dependence plots to assess how a random forest model predicts TSS concentrations in the Chesapeake Bay estuary using different spectral bands from MODIS satellite data. The results revealed that the blue band (496, 448 and 443 nm) was useful for estimating low TSS concentrations, while the green band (531 and 555 nm) became important for estimation when higher TSS concentrations were observed.

These studies (DeLuca et al. 2018; Loaiza et al. 2023a; Mpakairi et al. 2024) have shown that various methods (regression, random forest and PDPs) have been applied to determine and illustrate relationships between an input and output variable; hence, they can be considered as GSA regression-based approaches for sensitivity analysis. Xin-hui and Cai-lan, 2021) used spectral simulation experiments to perform a sensitivity analysis method when they evaluated how different sensor parameters – such as the spectral resolution, signal-to-noise ratio (SNR), and radiation resolution – influence the performance of water quality inversion models for remote sensing monitoring. To this end, previous studies focused on the prediction of water quality parameters, i.e. spectral reflectance as model input (explanatory variables), and explained their contribution to the uncertainty in estimating the water quality parameters (the output). While these studies determine which spectral bands are important for making accurate predictions, they do not directly provide information about the sensitivity of spectral bands to variability in water quality parameters. In the present study, our interest was to determine the sensitivity of the Sentinel-2 spectral bands to the variability in water quality parameters during high-flow (i.e. wet) and low-flow (i.e. dry) conditions in the Cradle of Humankind World Heritage Site (COHWHS), South Africa. This paper forms the first part of a series of studies investigating the sensitivity of Sentinel-2 data to spatial and temporal trends in surface water quality in water bodies in and around the COHWHS, with Ngamile et al. (2025) presenting the second part of the series. The results of this study were achieved using the Multiple Linear Regression, Random Forest variable importance and PDPs by modelling the relationship between multiple optically-active and non-optically active water quality parameters (i.e. input variables) with spectral reflectance per Sentinel-2 band (i.e. response). By establishing the relationship between the water quality parameters and water-leaving reflectance, the effect of water quality parameters on the variability of spectral reflectance in each band (i.e. how much the variation in spectral band reflectance or absorption patterns is due to changes in water quality parameters) can be established.

In this way, we can determine the degree to which variations in water quality parameters influence (or impact) the reflectance as recorded by Sentinel-2, thus the sensitivity of Sentinel-2 bands to such parameters. The specific objectives of this study were to: (1) determine if there are significant statistical differences in water quality parameters under high- and low-flow conditions, (2) analyze the bivariate relationships between water quality parameters and Sentinel-2 bands, and (3) assess the consistency of various sensitivity analysis techniques, i.e. multiple linear regression (MLR), random forest (RF), and partial dependence plots (PDPs), in determining the sensitivity of Sentinel-2 MSI bands to optically and non-optically active water quality parameters under high- and low-flow conditions.

2. Materials and methods

2.1. Description of the study area

The Cradle of Humankind World Heritage Site (COHWHS) is a trapezoidal area of approximately 800 km^2, located 40 km northwest of Johannesburg, within the West Rand District of Gauteng, South Africa. It was declared a UNESCO World Heritage Site in 1999 because of its significant palaeo-anthropological sites, including over 200 caves with fossilised remains of ancient life forms, particularly hominids (Durand and Meeuvis, 2010). However, the site is faced with environmental threats from acid mine drainage (AMD) resulting from the closure of mining operations in the gold-rich western Witwatersrand Basin, which has been mined since 1887 (McCarthy 2011). This pollution impacts local water bodies, including Tweelopiespruit (Dam [F11S12]), Blougatspruit (PSD and BB@N14), Bloubankspruit (BB@M and BB@NSP) and Cradlemoon Lake, which receive sediment inflow from the Crocodile River, affecting water quality in various parts of the area (Windisch et al. 2022). The site is located within the Crocodile (West) and Marico Water Management Area, specifically the upper Crocodile sub-management area, and lies in secondary drainage region A2 and tertiary drainage region A21. Pollution from mining, agricultural runoff, and municipal sewage leads to increased nutrient levels, bacterial contamination, and high nitrate and phosphate concentrations in rivers. This impacts downstream water users, including those relying on the Hartebeespoort Dam (Hobbs 2017).

2.2. Data collection

2.2.1. In-situ data collection

The in situ measurements of the water quality parameters, dissolved oxygen (DO), pH, temperature and electrical conductivity (EC), occurred on the 14^{th} and 16^{th} of March 2024 (i.e. wet season) and the 28th and 31st of August 2024 (i.e. dry season), representing high-flow and low-flow conditions, respectively. These dates were selected to correspond with the satellite overpass of Sentinel-2 MSI. All in situ measurements were taken between 09h00 SAST and 15h00 SAST to minimize the gap between the satellite overpass and in situ measurements. The water quality parameters were collected using the Hach HQ40d multiparameter meter by switching various probes designed to capture each parameter. A total of 40 single measurements of each water quality parameter were collected from six purposively selected sites (Figure 1). The sites were selected to represent different water bodies and potential pollution influences within the study area, while also considering accessibility for field sampling. At each site, measurement points were selected within specific sampling areas of the water bodies to capture variability. The coordinates of the sampling sites were recorded using a Garmin GPSMAP 65S handheld GPS device, which has a positional accuracy of ±3 m.

2.2.2. Laboratory analysis

At each sampling location for the in situ water quality parameters, water samples were also collected using 1-L water bottles at depths ranging between 10 cm and 0.5 m at each site, resulting in a total of 40 samples. The depth range was chosen to avoid collecting sludge, mud, and sand, especially from shallower water sources during low-flow conditions (i.e. dry season). The water samples were stored in a cooler box with ice cubes to maintain a low temperature and preserve the condition of the samples while in transit and stored in a cold room at the Hydrology and Water Resources Laboratory of the Council for Scientific and Industrial Research (CSIR) at 4 °C. The water samples were analyzed within 72 hours, with chlorophyll-*a* and suspended solids results released.

2.2.3. Satellite data

Sentinel-2 Level 1C images, which corresponded with the in situ measurement dates, were downloaded from the Copernicus Browser on the Copernicus Data Space Ecosystem (https://dataspace.copernicus.eu/). The images were atmospherically corrected using *i*COR on the Sentinel Application Platform (SNAP) software. The *i*COR software plugin is used to atmospherically correct spaceborne, airborne and drone images for atmospheric effects on land and inland, coastal and transitional waters (Wolters et al., 2021). After the atmospheric correction process, Sentinel-2 bands 1–8, 8A, 11 and 12 were resampled to 10 m

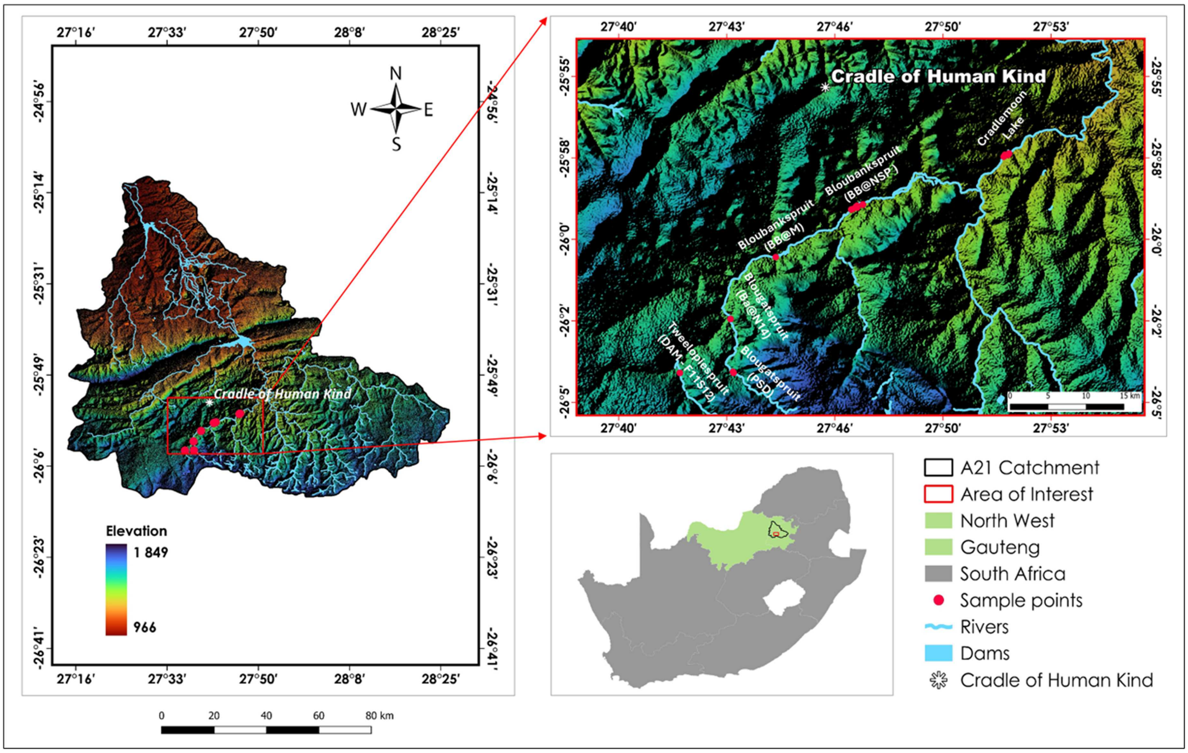

Figure 1. Location of the COHWHS within the A21 catchment area.

using the bilinear resampling technique and selected for further analysis. Bilinear interpolation was used because it provides smoother results for continuous spectral data as compared to nearest neighbour, which can introduce pixelation (Parsania and Virparia 2016). Finally, the pixel values (water-leaving reflectance) intersecting the locations (i.e. GPS coordinates) of the sampling sites were extracted in ArcGIS Pro for further analysis.

2.3. Bivariate analysis

Bivariate analysis was performed using Pearson's r correlation analysis (Equation (1)) to determine the relationship between each water quality parameter and the Sentinel-2 bands. The Pearson's r correlation coefficient measures the strength and direction of the linear relationship between two variables, x and y.

$$r = \frac{\sum_{i=1}^{n}(x_i - \bar{x})(y_i - \bar{y})}{\sqrt{[\sum_{i=1}^{n}(x_i - \bar{x})^2][\sum_{i=1}^{n}(y_i - \bar{y})^2]}}, \tag{1}$$

where x_i and y_i are the values of x and y for the i th observation. The Pearson correlation coefficient r was grouped into $0 \le r \le 0.2$ (very weak), $0.2 < |r| \le 0.4$ (weak), $0.4 < |r| \le 0.6$ (moderate), $0.6 < |r| \le 0.8$ (strong) and $0.8 < |r| \le 1.0$ (very strong) for interpretation purposes.

2.4. Sensitivity analysis techniques

The sensitivity analysis refers to the development of a mathematical model to determine how dependent a model output is on a model input or how a model input influences the model output (Razavi et al. 2021). This method was used in this study in order to determine the sensitivity of Sentinel-2 bands to optically and non-optically active water quality parameters. When using the sensitivity analysis method, the model input may refer to a model's parameter (water quality parameters), while the model output may refer to a model's response (Sentinel-2 band sensitivity). Three models were chosen to assess both simple and complex sensitivities across a range of optically and non-optically active water quality parameters. Between the input and the output, the MLR model can predict direct and linear relationships, the RF model can deal with complex and nonlinear interactions, and the PDP model can help with interpreting and visualising complex RF models. In this analysis, the study sought to establish spectral bands that are responsive to variations in the distribution of chlorophyll-*a*, suspended solids, dissolved oxygen (DO), pH, temperature and electrical conductivity (EC) across two seasons. The sensitivity analysis models were developed and performed on the *R Studio* software in order to identify which Sentinel-2 bands are most responsive to changes in both the optically and non-optically active water quality parameters.

2.4.1. Multiple linear regression

Regression is defined as a statistical tool that can be used to predict relationship(s) between a dependent variable and one or more independent variables (Yang 2017). Yang (2017) further stated that this method is widely used to predict and estimate the expected value of a dependent variable based on given independent variables, often intersecting with machine learning applications. Regression can be categorized as linear regression, non-linear regression and logistic regression. This study focused on linear regression, which has traditionally been categorized as two types of regression models: simple linear regression and multiple linear regression. Both are used to find a linear relationship between one or more predictors (Maulud & Abdulazeez 2020). Traditional methods of linear regression have focused on simple linear regression to understand relationships, as they assume that relationships are linear, but this approach may not work for non-linear or complex relationships (Razavi et al. 2021). Other traditional approaches have focused on multiple linear regression (MLR), which is used to model the relationship between a dependent variable and two or more independent variables (Kim et al. 2020).

MLR can fit a linear equation with multiple independent variables, which shows its flexibility in modelling complex real-world events across different datasets (Deniz 2020). Additionally, MLR has been used in water quality monitoring studies (Lavanya et al. 2024; Loaiza et al. 2023b; Yin et al. 2019) that use remote sensing techniques to understand and predict relationships between a dependent variable (such as water quality parameters) and multiple independent variables (such as meteorological conditions, land-use factors, and satellite sensor bands). Thus, this study used the MLR model to determine the sensitivity of Sentinel-2 bands to optically and non-optically active water quality parameters. To perform the sensitivity analysis, chlorophyll-*a*, suspended solids, DO, pH, temperature and EC were the independent variables, and each of the Sentinel-2 spectral bands was the dependent variable of the model. The model quantified the relationship using the coefficient of determination (R^2). The form of the model is shown in Equation (2) as follows:

$$y = C + \beta_1 x_1 + \beta_2 x_2 + \beta_1 x_1 \ldots \beta_k x_k, \tag{2}$$

where $\beta_{1\,(i=1,2,\ldots k)}$ represents a regression coefficient for the independent variable $x_{i\,(i=1,2,\ldots k)}$, y refers to the dependent variable, and C is the constant of the regression equation (Kim et al. 2020).

2.4.2. Random forest variable importance

Random forest is a machine learning algorithm that is widely used because of its ability to handle complex data, manage many independent variables at once, and capture nonlinear relationships between variables (Mpakairi et al. 2023). It makes predictions by building multiple decision trees and combining their results to improve accuracy and stability (Rodriguez-Galiano et al. 2012). There are various visualisation techniques in which random forest data can be presented, and one of these techniques is the use of the variable importance measure (VIM). Liu and Zhao (2017) stated that the VIM can be used to improve model performance by ranking feature importance, and it can be used to visualize important variables that contribute to output results. A random forest can measure how important each input variable is by using the VIM. This works by randomly mixing up the values of a variable and seeing how much the model's prediction accuracy decreases (Tami et al. 2018). If the error increases significantly, it means that the variable plays an important role in making accurate predictions (Boonprong et al. 2018). This ability to rank variables is useful in many applications because it helps researchers focus on the most influential factors, improving both model efficiency and interpretability. In this study, the random forest model was applied, and the VIM was used to visualize the results.

This method was applied to determine how water quality parameters influence Sentinel-2 spectral reflectance as part of the sensitivity analysis techniques. The Sentinel-2 bands were used as dependent variables, while water quality parameters served as independent variables. The output results (variable importance results) of the model were evaluated using the % mean increase in the mean squared error (MSE), which measures how important a variable is by checking how much the prediction accuracy drops when the values of that variable are randomly shuffled (Bonneu et al. 2024). If the accuracy decreases a lot, the variable is important; if it barely changes, the variable is not very useful for predictions (Bonneu et al. 2024). In addition to measuring the overall model performance, random forest also ranks the water quality parameters based on their importance in predicting changes in the Sentinel-2 bands. This ranking helps identify which parameters, such as chlorophyll-*a*, suspended solids, DO, pH, temperature and EC, have the strongest influence on spectral reflectance.

2.4.3. Partial dependence plots

The random forest model has also been applied in partial dependence plots (PDPs), particularly for visualizing the response surface. PDPs are visualization tools that are used in machine learning to provide valuable insights into model results (Sfravara et al. 2024). They are used to illustrate how one input (predictor) variable influences a model's output (prediction) results while keeping all other variables constant (Johnson et al. 2022). Additionally, this tool helps to isolate an individual input's effect (Sfravara et al. 2024). This method is particularly useful for interpreting complex, nonlinear relationships in data and is often used as a sensitivity analysis tool in predictive machine learning models, such as random forest (Ly et al. 2022). In the context of this study, PDPs were used to assess the sensitivity of Sentinel-2 bands to optically and non-optically active water quality parameters. By visualising the partial dependence of Sentinel-2 spectral bands on increases and decreases in the concentrations of chlorophyll-a, suspended solids, DO, pH, temperature, and EC, PDPs help illustrate how changes in these parameters influence spectral reflectance and band sensitivity.

Additionally, the random forest model was used to generate partial dependence (PD) contour plots, which quantify the combined effects of predictor variables (water quality parameters) on the response variable. This approach helps visualize how variations in predictor concentrations influence the output. Using this approach, an effective way to assess the marginal effects of two correlated variables simultaneously is through plotting their estimated probabilities in a contour plot (Shafiullah et al. 2019). This approach also helped to assess whether the relationships captured by the random forest model align with known physical and biochemical processes in the water bodies.

3. Results

3.1. Summary statistics of in situ and laboratory measurements

Tables 1 and 2 present the summary statistics for optically active and non-optically active water quality parameters, respectively, collected during high-flow (14 and 16 March 2024) and low-flow (28 and 31 August 2024) conditions. As shown in Table 1, the chlorophyll-*a* and suspended solids concentrations were higher during the high-flow conditions (i.e. wet season) relative to low-flow conditions (i.e. dry season). The coefficient of variation (CV) shows high variability in low- and high-flow conditions. During low-flow, the variability of chlorophyll-*a* was much higher than in the high-flow, indicating its sensitivity to changes in water flow. On the other hand, suspended solids also displayed notable variability during

Table 1. Summary statistics of optically active water quality parameters during high-flow (i.e. wet) and low-flow (i.e. dry) conditions.

	Parameter	Min.	Max.	Mean	Std. Dev.	CV (%)
High-flow	Chlorophyll-*a* (μg/L)	5	653	92.8	174.29	187.81
	Suspended solids (mg/L)	10	1543	222.25	357.39	160.80
Low-flow	Chlorophyll-*a* (μg/L)	5	382	45	101.03	224.51
	Suspended solids (mg/L)	8	549	124.65	158.05	126.8

Table 2. Summary statistics of non-optically active water quality parameters during high-flow (i.e. wet) and low-flow (i.e. dry) conditions.

	Parameter	Min	Max.	Mean	Std. dev.	CV (%)
High-flow	DO (mg/L)	0.1	7.92	3.48	2.88	82.76
	pH	5.55	8.01	7.31	0.57	7.80
	Temp (°C)	20.7	30	25.72	2.76	10.74
	EC (μs/cm)	226	2950	753.15	658.12	87.38
Low-flow	DO (mg/L)	0.43	21.86	7.67	6.20	80.84
	pH	4.44	10.57	8.12	1.26	15.52
	Temp (°C)	14.40	23.30	18.03	2.58	14.31
	EC (μs/cm)	268	2850	896	660.32	73.70

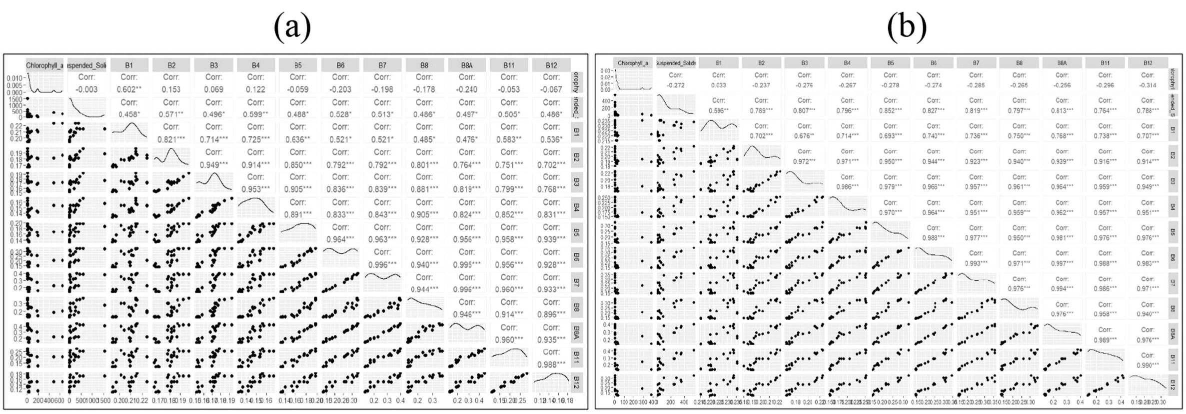

Figure 2. Pearson *r* correlation analysis results during the (a) high-flow and (b) low-flow conditions.

low-flow but it was higher during high-flow conditions, which was attributed to the increased runoff and substances in the water bodies.

In Table 2, the summary statistics results show relatively high minimum and maximum values of pH, temperature and EC under high-flow (i.e. wet) conditions, as compared to the results of low-flow (i.e. dry) conditions. This could be attributed to increased runoff caused by rainfall, which in turn brings and mixes different dissolved substances from surrounding land use, as well as seasonal warm weather (for temperature). This phenomenon causes an increase in pH, temperature and EC levels. However, the results for DO were different, showing relatively high minimum and maximum values under low-flow conditions. Low-flow (i.e. dry season) conditions are characterized by calmer water and decreased runoff; hence, water remains more stable and can hold more oxygen because of fewer substances in the water. In terms of the variability in water quality between the high-flow and low-flow conditions, the coefficient of variation (CV) for DO and EC was higher in the high-flow, while for pH and temperature, the CV was relatively higher under low-flow conditions. Generally, pH and temperature exhibited lower variability under the two flow conditions, compared to DO and EC.

3.2. *Bivariate analysis of water quality parameters and Sentinel-2 reflectance*

Pearson correlation analysis was conducted using combined data from all sampling sites for each flow condition (high-flow and low-flow) to evaluate the overall relationships between the water quality parameters and Sentinel-2 reflectance values. Figure 2(a) and (b) show the relationships between the optically active water quality parameters, i.e. chlorophyll-*a* and suspended solids, and the reflectance values of the Sentinel-2 bands under high-flow and low-flow conditions, respectively. Under high-flow conditions (Figure 2[a]), chlorophyll-*a* had a strong-positive correlation with B1 (i.e. coastal aerosol band), which was statistically significant ($p \leq 0.05$) at $\alpha = 0.05$, while having a very weak positive relationship with the other bands in the visible spectrum (i.e. B2–B4). For most bands in the red-edge (RE), near-infrared (NIR) and shortwave-infrared (SWIR) spectrum, the *r* coefficient was also in the very weak range;

however, in the negative direction (i.e. B5, B7, B8, B11, and B12). However, B6 (RE-2) and B8A (NIR-2) exhibited a weak negative relationship, i.e. $r \cong -2$. Under low-flow (i.e. dry) conditions (Figure 2[b]), chlorophyll-a showed a very weak negative correlation with most spectral bands and a weak negative relationship with B12, i.e. $r \cong -0.3$. However, chlorophyll-a exhibited a very weak positive relationship with B1. None of the correlations was statistically significant under low-flow conditions ($p > 0.05$).

In contrast, the suspended solids had a moderate-positive r correlation with all the Sentinel-2 bands during high-flow conditions. Under low-flow conditions, the suspended solids exhibited a strong positive relationship with the Sentinel-2 spectral bands in the visible portion of the electromagnetic spectrum (i.e. B2 and B4), NIR (B8) and SWIR (B11 and B12). Interestingly, a very strong-positive correlation was achieved with the green band (B3), the spectral bands in the red-edge bands, i.e. B5, B6, and B7 and the narrow NIR band, i.e. B8A. All r correlations under low-flow conditions were statistically significant at $\alpha = 0.05 \ (p \leq 0.05)$.

Figure 3(a) and (b) show the relationships between non-optically active water quality parameters, i.e. DO, pH, temperature and EC, and the reflectance values of the Sentinel-2 bands under high-flow and low-flow conditions, respectively. Under high-flow conditions (Figure 3[a]), DO exhibited a very strong negative correlation ($r > -0.8$) with most Sentinel-2 spectral bands, except for the coastal aerosol band (B1), where a strong negative relationship ($r \cong 0.6$) was evident. On the other hand, EC had very weak negative relationships with B3–B7, while NIR (B8–B8A) and SWIR (B11–B12) exhibited a very weak positive relationship. B1 and B2 relationship to EC was also negative; however, they were moderate and weak, respectively. pH exhibited a strong relationship with B1–B4, a moderate positive relationship with RE (B5–B7), NIR-1 (B8) and SWIR −1 (B11), while NIR-1 (B8A) and SWIR-2 (B12) exhibited a weak positive correlation. Temperature showed a weak relationship with coastal aerosol (B1) and visible region (B2–B4) bands, while the other bands had a very weak positive relationship, most of which were not statistically significant ($p > 0.05$). Under low-flow conditions (Figure 3[b]), DO had strong negative correlations with all Sentinel-2 bands, except B1, where it had a very weak correlation. All the correlations were statistically significant. Like in high-flow conditions, EC correlations were also mostly very weak but positive, except for B3, B4 and B8, where weak relationships were evident. The pH and temperature results indicate very weak and weak relationships in all the bands, with few variations in terms of the direction of the relationship. Moreover, none of the r correlations between these water quality parameters (i.e. pH and temperature) and Sentinel-2 bands were statistically significant.

3.3. Sensitivity analysis

The results of the sensitivity analysis using multiple linear regression (MLR), random forest regression (RF), and partial dependence plots (PDP) with partial dependence (PD) contour plots are presented in

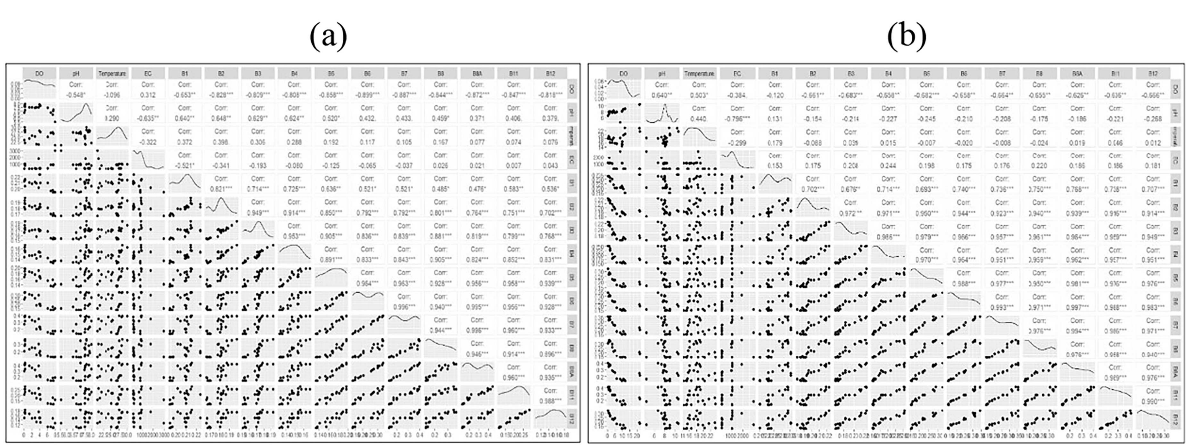

Figure 3. Pearson r correlation analysis results during the (a) high-flow and (b) low-flow conditions. The asterisks indicate the statistically significant correlations, where * represents $0.01 < p \leq 0.05$, ** represents $0.001 < p \leq 0.01$ and *** represents $0.001 < p \leq 0.01$.

subsections 3.3.1 and 3.3.2 for the optically active and non-optically active water quality parameters, respectively.

3.3.1. Optically active water quality parameters

The sensitivity of the Sentinel-2 spectral bands to the optically active water quality parameters (chlorophyll-*a* and suspended solids) was considered, where chlorophyll-*a* and suspended solids served as independent (predictor) variables and B1–B8, B8A, B11, and B12 served as dependent (response) variables. The results for the MLR, RF and PDP techniques are presented in Figures 4 and 5, respectively, while Figures 6 and 7 illustrate PDPs' results. The results varied by bands, the modelling approach, and the flow condition. Figure 4(a) shows that under high-flow (i.e. wet season) conditions, chlorophyll-*a* had a relatively low influence on the Sentinel-2 spectral bands ($R^2 < 0.1$), except for B1 (i.e. coastal aerosol band), where it explained more than 35% of the reflectance variability in this band ($R^2 > 0.35$). Under low-flow (i.e. dry season) conditions (Figure 4[b]), chlorophyll-*a* followed a similar trend across most Sentinel-2 bands, except for B1, where its influence on the reflectance was too low, i.e. R^2 values close to 0. The suspended solids, on the other hand, indicated a consistent trend across all spectral bands in both flow conditions, with R^2 values higher than those of chlorophyll-*a* for most bands (excluding B1 under high-flow conditions). Under high-flow conditions (Figure 4[a]), suspended solids explained the highest variability of more than 35% in the reflectance of B2 and B4, while they also explained approximately 20%–25% of the variability in the remaining Sentinel-2 bands. However, under low-flow conditions Figure 4[b]), this water quality parameter explained most of the variability in the reflectance of all Sentinel-2 bands, explaining variability over 60%, i.e. $R^2 > 0.6$, except B1 and B11, where the R^2 values were ~35% and ~58%. Notably, B5 was mostly affected by suspended solids, explaining 70% of the reflectance variability in this band.

Figure 5 shows the RF variable importance of the optically active water quality parameters (predictors) for each Sentinel-2 band (response) under high-flow and low-flow conditions. Generally, the results show that chlorophyll-*a* had relatively low importance in predicting Sentinel-2 reflectance under both flow conditions. Under high-flow conditions (Figure 5[a]), the chlorophyll-*a* importance values were close to 0 for B2 and B5 and negative for B3. In contrast, under low-flow conditions (Figure 5[b]), the influence of chlorophyll-*a* on the Sentinel-2 spectral bands was rather stable, with variable importance values higher than those observed under high-flow conditions. Somewhat notable influences on reflectance, i.e. >10%, can be seen for B6, B7, B8A, B11 and B12, while it had relatively low importance, i.e. <10%, is observed in other bands. Similar to the MLR results, the suspended solids showed higher variable importance values than chlorophyll-a across all the Sentinel-2 bands under both flow conditions. This influence was more evident in B1–B6 and B11 under high-flow conditions (Figure 5[a]), where the importance was ≅30%, while similar importances were observed in B2–B5, B8 and B8A under low-flow conditions, although these values were slightly lower, i.e. ≅25%. In the other spectral bands, suspended solids had an importance

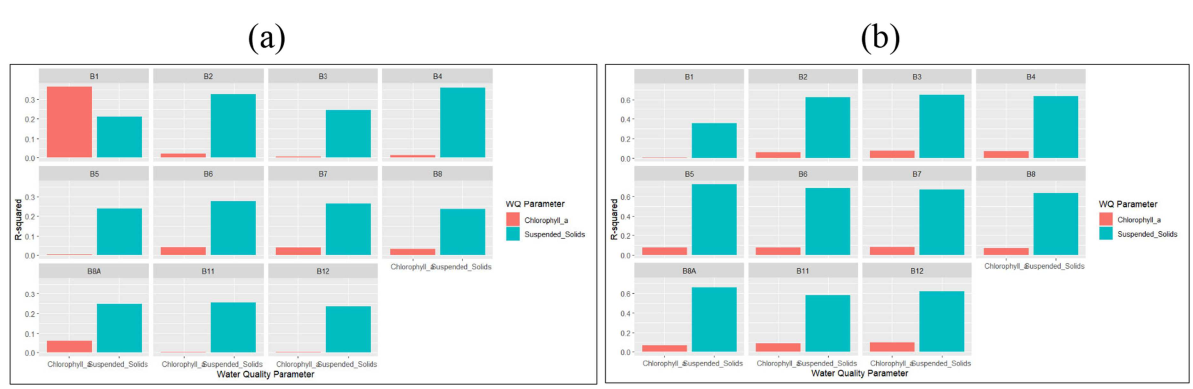

Figure 4. Sensitivity analysis of Sentinel-2 spectral bands to optically active water quality parameters using the multiple linear regression (MLR) model under (a) high-flow (i.e. wet) and (b) low-flow (i.e. dry) conditions. The units of the input variables shown on the x-axis in each plot are as follows: chlorophyll-*a* (µg/L) and suspended solids (mg/L).

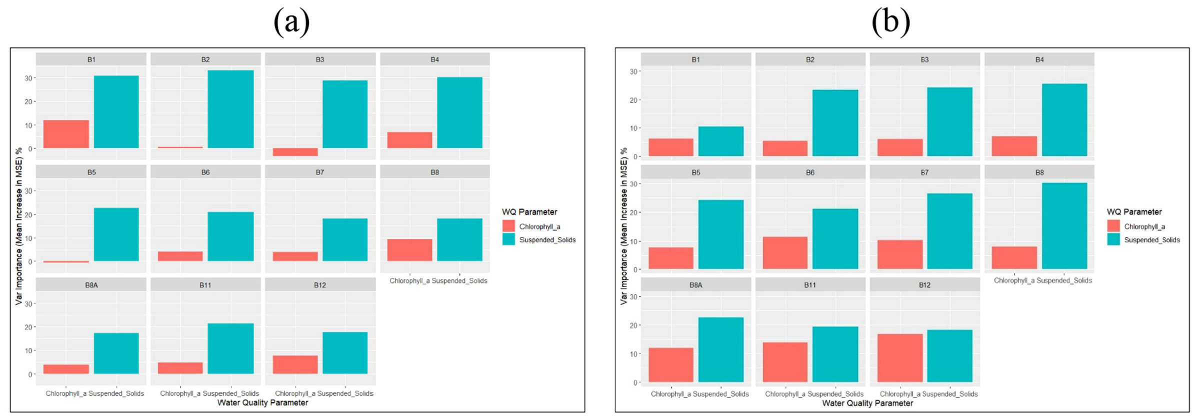

Figure 5. Sensitivity analysis of Sentinel-2 spectral bands to optically active water quality parameters using the random forest (RF) model under (a) high-flow (i.e. wet) and (b) low-flow (i.e. dry) conditions. The dry condition variables shown on the x-axis in each plot are as follows: chlorophyll_*a* (μg/L) and suspended solids (mg/L).

value of ≅20% under both flow conditions, except for B1 under low-flow conditions, where the importance was approximately 10%.

Although the results between MLR and RF were generally consistent, it is important to note that these models inherently capture the variable interaction, where a water quality parameter may appear important not only for its direct contribution but also due to interaction with other parameters. Therefore, it is crucial to assess the marginal effect of one parameter while the others are held constant. To achieve this, we used partial dependence plots (PDPs), and the results are presented in Figures 6 and 7. In Figures 6 and 7, it is shown that the influence of chlorophyll-*a* on the Sentinel-2 reflectance varied with flow conditions, whereas under high-flow (i.e. wet) conditions, it was more pronounced in the visible region of the electromagnetic spectrum, while the influence was negligible under low-flow (i.e. dry) conditions. Under high-flow conditions (Figure 6), the coastal aerosol band (B1) showed high sensitivity to chlorophyll-*a* concentrations ranging from approximately 300 to 600 μg/L, while concentrations ranging from 50 to 350 μg/L showed moderate sensitivity.

In B2, chlorophyll-*a* concentrations of about 50 μg/L caused a reduction in reflectance, while concentrations ranging from 100 to 550 μg/L caused a slight increase in reflectance, and values greater than 550 μg/L caused a marginal increase in reflectance. Similar to B1, B4 showed increased sensitivity when the chlorophyll-*a* concentration increased above 350 μg/L. However, the increase in reflectance resulting from these concentrations was rather low. The other Sentinel-2 bands, i.e. B3 (visible spectrum), B5 and B7 (red edge), B8 and B8A (NIR), and B11 and B12 (SWIR), were more sensitive to relatively low chlorophyll-*a* concentrations (i.e. <250 μg/L), while B6 (red edge) and B8A (narrow NIR), showed sensitivity to chlorophyll-*a* concentrations of up to 400 μg/L. Under low-flow conditions (Figure 7), the chlorophyll-*a* concentrations were relatively low, but the Sentinel-2 bands were sensitive to certain ranges. Notably, chlorophyll-*a* concentrations >200 μg/L caused a marked increase in reflectance in B1 (coastal aerosol band), while other bands showed similar trends but with a relatively minute influence on reflectance.

In contrast, the sensitivity of Sentinel-2 to suspended solids under both flow conditions differed significantly from that of chlorophyll-*a*, strongly influencing spectral reflectance across all bands. Suspended solids concentrations between 100 and 500 mg/L explained the greatest variability in all Sentinel-2 bands under high-flow conditions, while concentrations above 500 mg/L resulted in spectral saturation, where the reflectance showed little change despite further increases in suspended solids at very high concentrations (Jaywant and Arif 2024; Joshi et al. 2025). Under low-flow conditions, the trend remained consistent across all spectral bands, although suspended solids concentrations were lower. The Sentinel-2 bands were more sensitive to suspended solids concentrations ranging from 50 to 400 mg/L, which explained the greatest variability in the reflectances of most bands except for B1, where concentrations above 200 mg/L resulted in low variability in reflectance.

Figure 6. Partial dependence plots (PDPs) for sensitivity analysis during high-flow (i.e. wet) conditions. The units of the input variables shown on the x-axis in each plot are as follows: Chlorophyll_*a* (μg/L) and suspended solids (mg/L).

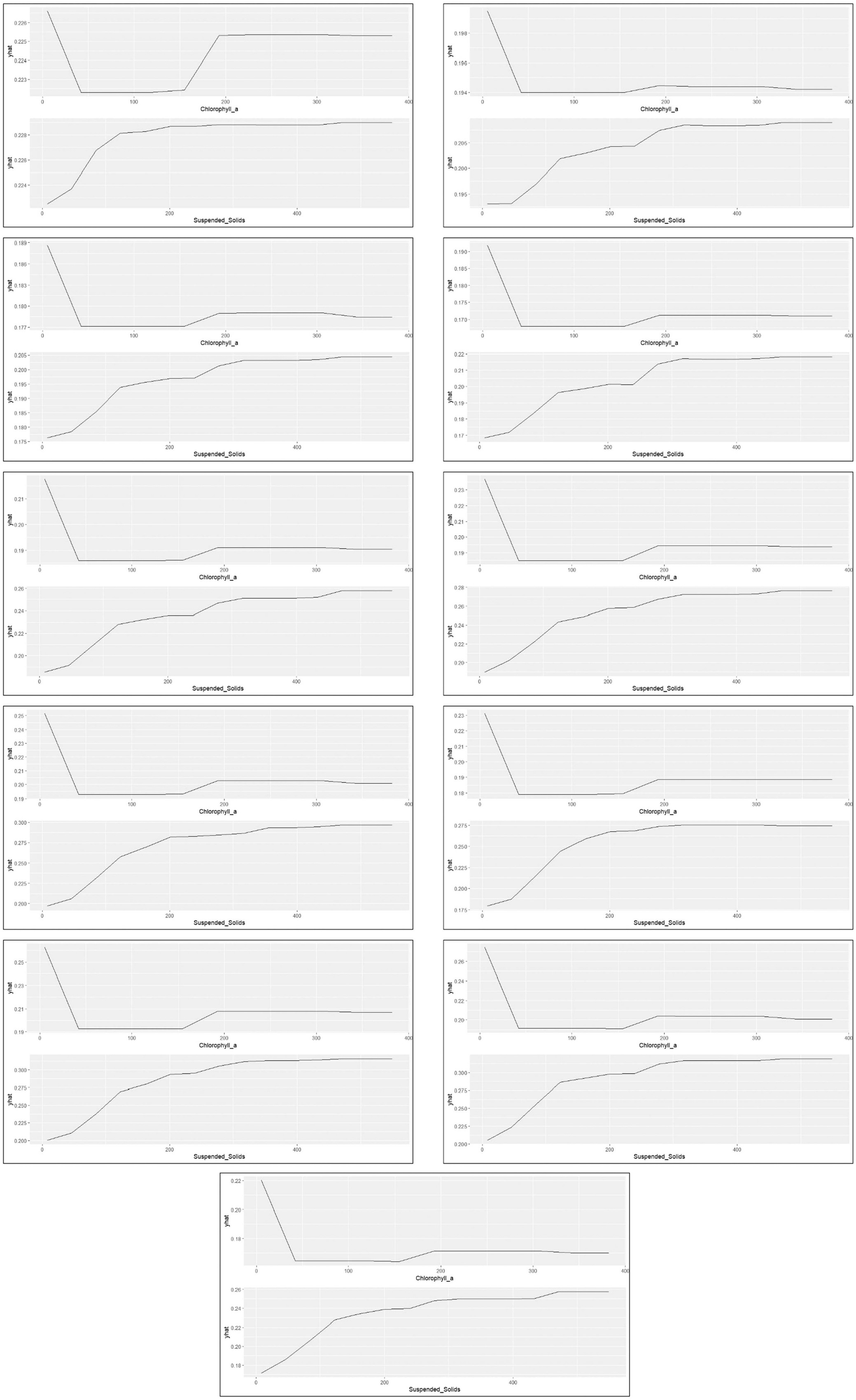

Figure 7. Partial dependence plots (PDPs) under low-flow (i.e. dry) conditions. The units of the input variables shown on the x-axis in each plot are as follows: chlorophyll_*a* (μg/L) and suspended solids (mg/L).

3.3.2. Non-optically active water quality parameters

In addition to optically active parameters (i.e. chlorophyll-*a* and suspended solids) in 3.3.1, we sought to determine the sensitivity of the Sentinel-2 bands to various non-optically active water quality parameters, i.e. DO, EC, pH, and temperature. To achieve this goal, we used MLR, RF, and PDPs to evaluate the relationships between multiple non-optically active water quality parameters (i.e. input variables) with each of the Sentinel-2 bands (i.e. response) under high-flow (i.e. wet) and low-flow (dry) conditions. Figure 8 presents the sensitivity results of Sentinel-2 spectral bands to non-optically active water quality parameters (DO, EC, pH, and Temperature) using R^2 values derived from multiple linear regression (MLR). Under both high-flow and low-flow conditions, DO explained the highest variability in Sentinel-2 reflectance across all bands, i.e. R^2 values > 60% and >40%, under the corresponding flow conditions. However, the amount of variability explained in B1 was the lowest across all flow conditions considered, i.e. $R^2 < 5\%$. On the other hand, pH explained the greatest variability in B1–B4 reflectance, i.e. $R^2 \cong 40\%$ under high-flow conditions, while it explained <30% in reflectance variability in other bands (Figure 8[a]).

Under low-flow conditions (Figure 8[b]), the influence of pH significantly decreased, with its highest R^2 value of only approximately 7% observed in B12. Temperature showed a relatively low influence on Sentinel-2 reflectance across bands and under both flow conditions. Most of its effect, explaining only 9%–12% of the variability in reflectance, was evident in B1–B4. Its influence in other bands was negligible, explaining <2% of the reflectance variability. Under low-flow conditions, temperature was even less influential across all Sentinel-2 bands, explaining <3% of the reflectance variability was only in B1. Similar to DO and pH, EC explained the greatest variability in the reflectance of the visible bands, i.e. mostly B1–B3, under high-flow conditions, with R^2 values of ~28%, ~11% and <5%, respectively. Under low-flow conditions, EC explained only 5% of the variability in reflectance across all the bands. Overall, the MLR results highlight that all Sentinel-2 bands are highly sensitive to DO concentrations, while their sensitivity for other non-optically active parameters depended on flow conditions (i.e. season) and the spectral region.

Figure 9 shows the importance values of different non-optically active water quality parameters, DO, EC, pH, and temperature (i.e., predictors), in explaining Sentinel-2 reflectance (i.e. response) under high-flow (i.e. wet) and low-flow (i.e. dry) conditions. Similar to MLR results in Figure 8, the RF variable importance results show that DO has the highest importance in predicting reflectance across all Sentinel-2 bands under both high-flow and low-flow conditions. Under high-flow conditions, the variable importance values were ≥30% in B7, B8A, and B11. Similar RF variable importance values were achieved for B2, B3, B5–B8, BA and B11–B12 under low-flow conditions. Temperature showed higher importance under high-flow conditions, with variable importance values >10% in the visible spectrum (i.e. B1–B4), while its importance in other bands was relatively low, i.e. <10%. In contrast, the RF variable importance of temperature was significantly low under low-flow conditions, with negative importance values recorded in B1, B2, B6–B8 and B8A. Notably, B11 showed no influence of temperature on its reflectance.

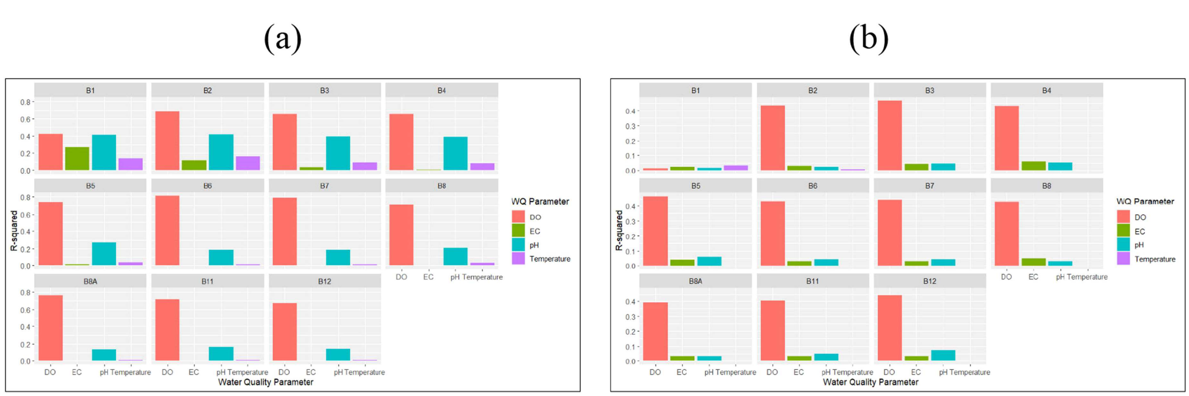

Figure 8. Sensitivity analysis of Sentinel-2 spectral bands to non-optically active water quality parameters using the multiple linear regression (MLR) model under (a) high-flow (i.e. wet) and (b) low-flow (i.e. dry) conditions. The units of the input variables shown on the x-axes are as follows: DO (mg/L), pH (unitless), temperature (°C) and EC (µS/cm).

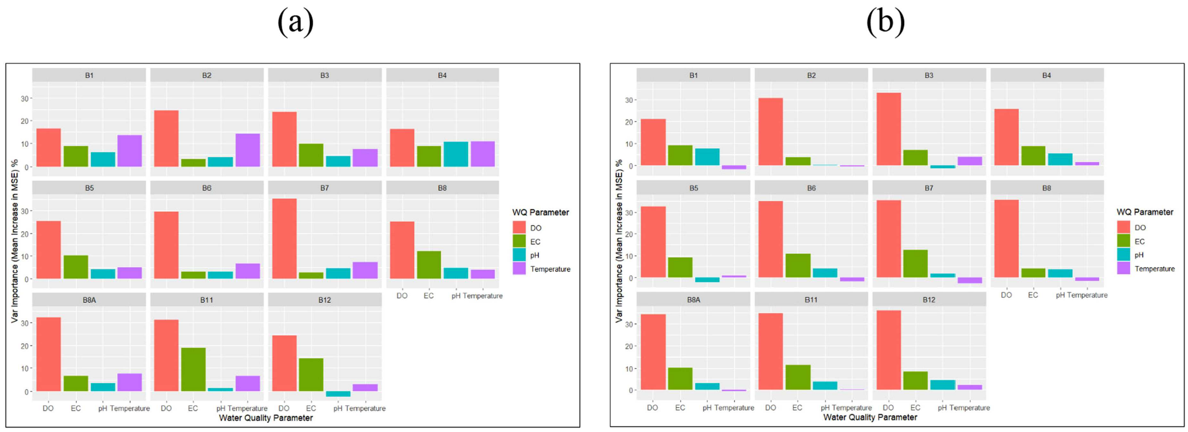

Figure 9. Sensitivity analysis of Sentinel-2 spectral bands to non-optically active water quality parameters using the random forest (RF) model under (a) high-flow (wet season) and (b) low-flow (i.e. dry) conditions. The units of the input variables shown on the x-axes are as follows: DO (mg/L), pH (unitless), temperature (°C) and EC (µS/cm).

EC exhibited the highest RF variable importance in predicting the water-leaving reflectance in B11, followed by B12, then B8 and B5, all of which showed importance >10% under high-flow conditions in the study area. Under these conditions, it was also important in explaining the reflectance variability across all the other Sentinel-2 bands, but its RF variable importance was relatively low, i.e. >5%, except for B2, B6 and B7. However, under low-flow conditions, the variable importance of EC in B6 and B7 was relatively high (i.e. >10%), which is different from the importance values recorded under high-flow conditions. Similar to high-flow conditions, B11 also exhibited variable importance >10%. In general, EC showed higher RF variable importance in several spectral bands, ranking second to DO in most cases. Conversely, pH had the least overall variable importance among all other water parameters under high-flow conditions, with a notable negative importance value recorded in B12. The highest variable importance value under these conditions was observed for B4, i.e. ~10%. Under low-flow conditions, pH exhibited relatively lower RF variable importance when compared to high-flow conditions. However, it was higher than the variable importance of temperature in most Sentinel-2 bands, except in B3 and B5. pH had negative variable importance in B3 and B5, while it had the highest importance in B1.

Partial dependence plots (PDPs) were computed to further explain the sensitivity of Sentinel-2 to non-optically active water quality parameters. As a model-agnostic technique, PDPs were computed on RF models to reveal the marginal effect of one water quality parameter on Sentinel-2 reflectance while averaging out the influence of other parameters. Hence, PDP analysis helps in disentangling the interactions of the water quality parameters within the model, highlighting the marginal effect of one water parameter on the reflectance. The results are presented in Figures 10 and 11. Table 2 shows that the DO concentrations measured under high-flow (wet season) conditions were lower (0.10–7.92 mg/L) compared to concentrations under low-flow (i.e. dry) conditions (0.43 –21.86 mg/L). Owing to these differences in concentrations across the two flow conditions (i.e. seasons), Figure 10 indicates that DO concentrations between 0 and 4 mg/L caused high reflectance, while concentrations of >4 mg/L resulted in declining reflectance in B1 to B4 under high-flow conditions. Beyond the visible portion, i.e. red-edge (B5–B7), NIR (B8 and B8A) and SWIR (B11 and B12), the reflectance started decreasing at concentrations around 2 mg/L. Under low-flow conditions (Figure 11), all Sentinel-2 bands were sensitive to DO concentrations >5 mg/L, while lower concentrations caused higher reflectance. B1 was also sensitive to DO concentration values >~17 mg/L, making the marginal effects in this band complex.

pH levels under high-flow conditions were also lower (i.e. 5.55–8.01) compared to low-flow conditions, i.e. 4.44–10.57 (see Table 2). Under high-flow conditions, all Sentinel-2 bands were responsive to higher pH levels, >7, which resulted in steadily increasing water-leaving reflectance. Contrasting results can be observed under low-flow conditions (Figure 11), where the relationship of pH with the spectral bands was more complex, as it resulted in higher reflectance in all bands when the pH was between 5.5 and 8 but declined when the pH exceeded 8. Regarding Temperature, its relationship with the spectral bands showed

Figure 10. Partial dependence plots (PDPs) showing the sensitivity of Sentinel-2 bands to non-optically active parameters under high-flow (i.e. wet) conditions. The units of the input variables shown on the x-axes are as follows: DO (mg/L), pH (unitless), temperature (°C) and EC (µS/cm).

Figure 11. Partial dependence plots (PDPs) showing the sensitivity of Sentinel-2 bands to non-optically active water quality parameters under low-flow (i.e. dry) conditions. The units of the response variables on the x-axes are as follows: DO (mg/L), pH (unitless), temperature (°C) and EC (μS/cm).

similar trends for all spectral bands under high-flow conditions. The temperature was relatively high under these conditions (which are consistent with the summer/wet season), i.e. 20.7 °C–30 °C, compared to the low-flow conditions, i.e. 14 °C–23.30 °C, corresponding to the winter/dry season. The Sentinel-2 spectral bands were not responsive to temperatures between 20 °C and 27.5 °C, causing only a little influence on the water-leaving reflectance. However, when the temperature rose beyond 27.5 °C, the reflectance increased. Under low-flow conditions, the Sentinel-2 bands were sensitive to water temperatures ranging between 16 °C and 20 °C; beyond this, reflectance in all the bands was invariant. Finally, Sentinel-2's sensitivity to EC (i.e. an indicator of total dissolved solids [TDS]) was consistent between the two flow conditions (i.e. seasons), attributed to similar EC levels under high-flow (226–2950 μS/cm) and low-flow (268–2850 μS/cm) conditions, respectively. EC levels between 1000 and 3000 μS/cm resulted in low reflectance in B1 under high-flow conditions but high reflectance under low-flow conditions. All the other Sentinel-2 bands affected the same for EC levels >1000 μS/cm under both high-flow (i.e. wet season) and low-flow (i.e. dry season) conditions.

4. Discussions

The sensitivity of the new generation sensors, such as Sentinel-2, to various optically and non-optically active water quality parameters is critical to determine its robustness and potential for spatial and temporal characterization of such parameters. This study sought to: (1) determine if there is a significant statistical difference in water quality parameters under high- and low-flow conditions, (2) analyze the bivariate relationships between water quality parameters and Sentinel-2 bands, and (3) assess the consistency of various sensitivity analysis techniques, i.e., multiple linear regression (MLR), random forest (RF), and partial dependence plots (PDPs), in determining the sensitivity of Sentinel-2 MSI bands to optically and non-optically active water quality parameters under high- and low-flow conditions within the Cradle of Humankind World Heritage Site (COHWHS).

4.1. Sensitivity of Sentinel-2 spectral bands to optically active water quality parameters

Optically active water quality parameters are recognized for their unique spectral characteristics within specific wavelength ranges of the electromagnetic spectrum. These parameters influence the reflectance and absorption properties of water, enabling satellite sensors to identify and detect them based on their spectral signatures (Adjovu et al. 2023a). To assess the sensitivity of Sentinel-2 spectral bands to optically active water quality parameters, this study focused on two key indicators: chlorophyll-*a* and suspended solids. According to Saberioon et al. (2020), chlorophyll-*a* and suspended solids are important indicators of the health of inland waters, making it essential to continuously monitor their changing concentrations. By leveraging Sentinel-2's high spatial and temporal resolutions, this study demonstrated that some spectral bands may be critical in characterizing the spatiotemporal variabilities of water quality. The statistical results revealed that suspended solids concentrations consistently had a stronger influence on spectral reflectance across all bands compared to chlorophyll-*a* under both high-flow and low-flow conditions. This dominance can be attributed to runoff from surrounding anthropogenic activities within the COHWHS, mainly the raw sewage discharge into water bodies, which caused an increase in suspended solids in the water. This, in turn, reduced chlorophyll-*a* concentrations by limiting photosynthesis rates (Durand and Meeuvis, 2010; Fanela and Takarina 2019).

Under low-flow (i.e. dry) conditions, the presence of chlorophyll-*a* from some water bodies influenced the results, hence, it was dominant, offsetting the overall effect of relatively lower suspended solids concentrations. The correlation analysis between the Sentinel-2 spectral bands and the two water quality parameters showed that the suspended solids had a strong positive correlation with all the Sentinel-2 bands under low-flow (i.e. dry) conditions while exhibiting moderately positive *r* correlations under high-flow (i.e. wet) conditions. This difference was attributed to increased turbidity under high-flow conditions caused by elevated levels of suspended solids (Ndou 2023). Higher turbidity introduces a complex mixture of particles that strongly scatter light in multiple directions, increasing background reflectance and masking the absorption features of chlorophyll-a. As a result, the chlorophyll-a signal becomes less detectable, reducing spectral clarity and weakening the correlation results (Cao and Li 2018; Fendereski et al. 2024b; Zhang and Wu 2026). While the suspended solids in other studies (Jiang et al. 2023; Ndou 2023) were mainly constituted by sediments, in our study, raw sewage and related sludge were dominant. Although high concentrations were observed under high-flow (i.e. wet) conditions, the presence of a high volume and velocity of water slightly reduced their relationship with the reflectance, while lower volumes and velocities under low-flow (i.e. dry) conditions allowed better sensing of the conditions by Sentinel-2, yielding strong relationships with spectral bands. This finding is consistent with that of Pasaribu et al. (2024), who noted that high current speeds in water increase the suspended solids concentration due to mixing, which lifts bottom materials and increases turbidity. Typically, the higher the suspended solids concentration, the higher the water-leaving reflectance (Xiao et al. 2023).

As illustrated in the results, the high sensitivity of Sentinel-2 bands to suspended solids indicates that this parameter plays a key role in controlling the optical properties of water in the study area while also highlighting the potential of these bands for its spatial and temporal estimation. This finding is consistent with those of previous studies (Caballero et al. 2018; Liu et al. 2017; Pasaribu et al. 2024) that showed that specific Sentinel-2 bands, particularly those in the visible and NIR regions, can effectively estimate suspended solids concentrations. Under wet (i.e. high-flow) conditions, our results showed that B2 and B4 stand out as highly sensitive bands, which is consistent with Amran and Daming (2023), who found that turbidity is highly correlated with the Sentinel-2 red band (B4). The RF results were generally consistent with the MLR results, indicating importance values ≅30% and ≅25% in most bands under high- and low-flow conditions, respectively. The RF-based partial dependence plots (PDPs) showed that suspended solids concentrations between 100–500 mg/L and 50–400 mg/L explained the greatest variability in all Sentinel-2 bands under high-flow and low-flow conditions, respectively (see Figures 5 and 6). To support this using RF-based PDPs, DeLuca et al. (2018) found that the red and near-infrared bands were the most important for predicting high concentrations of suspended solids, while blue and green bands in the visible spectrum were better at estimating low concentrations. Their study also showed that other bands, such as the 412, 443, and 547 nm bands of MODIS, contributed very little to the prediction results.

In contrast, chlorophyll-*a* was strongly positively correlated with the coastal aerosol band only (i.e. B1, located in the blue region) under high-flow (i.e. wet) conditions, while under low-flow (i.e. dry) conditions, a very weak positive correlation with this band was observed. The blue region is generally known for its high absorption characteristics of chlorophyll-*a*; therefore, this study reveals that the narrower Sentinel-2 Blue band (B1) is more related to chlorophyll-*a*. The sensitivity analysis results using MLR showed that chlorophyll-*a* explained 35% of the reflectance variability in this band, which was higher than the influence of suspended solids, underscoring the importance of B1 as a potential critical band for estimating chlorophyll-*a* spatially, especially during the wet season (i.e. under high-flow conditions). The PDPs showed that B1 was more sensitive to chlorophyll-*a* concentrations ranging from 300 μg/L to 600 μg/L under high-flow conditions, while >200 μg/L chlorophyll-*a* concentrations caused a marked increase in B1. According to Jang et al. (2024), phytoplankton containing chlorophyll-*a* absorbs light in the blue wavelength range (which includes B1). On the other hand, the RF results showed some influence of chlorophyll-*a*, >10% on spectral bands such as B6, B7, B8A, B11 and B12 under low-flow conditions, while this was the case for B1 and B8 only under high-flow conditions. However, the PDPs revealed that these bands were sensitive to low chlorophyll-*a* concentrations (i.e. <250 μg/L), except for B6 and B8A, which were sensitive to concentrations up to 400 μg/L. These spectral bands could be considered for mapping the spatial and temporal distributions of chlorophyll-*a* concentration in the future.

Studies such as Llodrà-Llabrés et al. (2023) and Mpakairi et al. (2024) have noted that the red-edge bands are effective for estimating chlorophyll-*a* in water bodies because of their known sensitivity to vegetation and plant health. Despite relatively low chlorophyll-*a* concentrations under low-flow conditions, the RF results showed consistent results with previous studies, ascertaining their usefulness. In the COHWHS area, the higher concentrations of suspended solids in most water bodies overshadowed the chlorophyll-*a* signal and lower chlorophyll-*a* concentrations. Interestingly, the RF model showed a negative influence of chlorophyll-*a* on B3, which is contrary to some studies (Arora and Mudaliar 2022; Viso-Vázquez et al. 2021) that found it effective for detecting chlorophyll-*a*. However, other studies, such as Fendereski and Creed, 2024a, 2024b), note that this only applies to deeper, clearer, and less turbid waters. In our study area, highly turbid conditions exist for most water bodies, primarily due to raw sewage and sewage sludge containing suspended solids. This turbidity interfered with the reflectance captured by B3, making it difficult to isolate the chlorophyll-*a* signal. Under low-flow conditions, however, the reduced presence of suspended solids in most water bodies altered the results. This reduction allowed chlorophyll-*a*-dominated water bodies to exert a greater influence on spectral band sensitivity as its signal became more prominent. Savoy and Harvey (2023)found that increasing chlorophyll-*a* also led to increasing turbidity in water. Similarly, Cheng et al. (2013) found that an increase in turbidity (caused by chlorophyll-*a* and the amount of suspended solids in water) led to a lower spectral signature of chlorophyll-*a* presence. In this study, the PD contour plots (Figure S1) further revealed that under high-flow (i.e. wet) conditions, chlorophyll-*a* ensitivity in the spectral bands was dependent on suspended solids concentrations ranging from 500 mg/L to 1500 mg/L. Conversely, suspended solids sensitivity was influenced when the chlorophyll-*a* concentration was less than 200 µg/L. In contrast, the reduced concentrations of suspended solids under low-flow (i.e. dry) conditions allowed the Sentinel-2 bands to detect the chlorophyll-*a* signal more effectively (see Figure S2 in the supplementary document).

4.2. Sensitivity analysis of Sentinel-2 bands to non-optically active water quality parameters

Research on the remote sensing of non-optically active water quality parameters remains limited because of their weak optical signals and low signal-to-noise ratio (Li et al. 2023). However, their interactions and co-occurrence with optically active parameters can influence the reflectance, making it important to assess their sensitivity to sensors such as the Sentinel-2. To address this gap in monitoring non-optically active water quality parameters, this study analyzed the sensitivity of Sentinel-2 bands to four non-optically active WQPs (i.e. DO pH, temperature and EC) using bivariate correlation analysis, MLR, RF variable importance and PDPs. The correlation results revealed that DO was strongly negatively correlated with all Sentinel-2 bands except for the coastal aerosol band (B1) under both high-flow and low-flow conditions. This can be attributed to how DO has a relationship with some of the parameters assessed in our study (chlorophyll-*a*, suspended solids and temperature). Increased concentrations of suspended solids and higher temperatures contribute to decreased DO, while chlorophyll-*a* increases DO through photosynthesis under high-flow conditions. As a result, the presence of these parameters, along with flow-induced mixing, can cause Sentinel-2 to inversely detect DO reflectance (Adjovu et al. 2023b; Guo et al. 2024; Hutchings et al. 2024). Sentinel-2 does not directly measure DO, but it captures optical signals influenced by chlorophyll-*a* and suspended solids, which all correlate with DO as an optically active water quality parameter.

On the other hand, pH showed strong positive correlations with visible region bands and red-edge 1, particularly under high-flow conditions. Poursanidis et al. (2019) stated that chlorophyll-*a* presence increases pH levels as photosynthesis consumes carbon dioxide, reducing carbonic acid and increasing pH. The Sentinel-2 bands B2 and B4 are associated with chlorophyll-*a* absorption, while B3 corresponds to its reflectance peak, and B5 is sensitive to chlorophyll-*a* content (Beal and Özdoğan 2024; Guo et al. 2023). This could explain the correlation between pH and these bands under high-flow conditions. These results suggest that DO and pH variations may influence optical properties through interactions with dissolved substances or chemical changes in the water. Temperature and EC correlation results were observed in the coastal aerosol band (B1), with a positive moderate correlation for temperature and a strong negative correlation for EC under high-flow (i.e. wet) conditions. This can be attributed to how EC measures dissolved ions that are diluted under high-flow conditions (Oyem et al. 2014). Sentinel-2 B1 is known for detecting aerosols (which may contain inorganic components), and it may be limited in its ability to detect dissolved ions; dilution reduces EC while affecting B1 reflectance, leading to a negative correlation (Lolli et al. 2024; Wu et al. 2018). Temperature is usually predicted using thermal bands from satellite sensors such as Landsat ETM+, which provide thermal infrared data at a spatial resolution of 60 m (Nasseri et al. 2023).

However, our results showed that temperature had a positive moderate correlation with B2 and B3 in the visible region under high-flow (i.e. wet) conditions. This effect can be attributed to how water surfaces reflect light, known as sun glint (Brown et al. 2021). Satellite bands detect glints more prominently under high temperatures because the sun's rays are more intense, and calm water surfaces enhance specular reflection, directing sunlight toward the viewer (Ottaviani et al. 2008). To further assess the sensitivity of the Sentinel-2 bands to DO, pH, temperature and EC, our study used MLR, RF variable importance and The results from these regression models revealed DO to be the most influential parameter in determining spectral band sensitivity under both high-flow and low-flow conditions. The visible region (B2–B4), RE (B5–B7), NIR (B8–B8A) and SWIR bands (B11–B12) were revealed to have the highest variable importance results for DO under both high-flow and low-flow conditions. This can further be attributed to DO's relationship with chlorophyll-*a* and suspended solids. DO's strong relationship with chlorophyll-*a* and suspended solids may have contributed to these results, particularly because the Sentinel-2 RE bands are sensitive to chlorophyll-*a* reflectance, while the visible region and NIR bands have been used to estimate suspended solids (Bramich et al. 2021; Saberioon et al. 2020). This is further supported by Salas and Kumaran, 2022, who measured DO on the Little Miami River in Ohio, where they found that the random forest model was effective in estimating DO concentrations with B5 (vegetation red edge) and B8 (near-infrared) on Sentinel-2.

For the remaining parameters – EC, pH, and temperature – the MLR and RF models produced varying results. The MLR results revealed that pH was observed to have a moderate influence on spectral band sensitivity under high-flow conditions in the coastal aerosol band and visible region bands. Studies such as Ndou (2023) (used Sentinel-2) and Abdelmalik (2018) (used Aster data) have found that the near-infrared bands to be more sensitive to pH, yet our study revealed the opposite results. This can be attributed to the relationship between pH and chlorophyll-*a*, as Arora et al. (2022) also found that chlorophyll-*a* concentrations strongly absorb light in the blue (B2 – 490 nm) and red (B4 – 665 nm) wavelengths while reflecting light in the green (B3 – 560 nm) and near-infrared (842 nm) wavelengths. This may have made these Sentinel-2 bands sensitive to pH. More results from the sensitivity analysis regression models revealed that the RF model showed Temperature and EC's moderate influence on spectral band sensitivity to be more pronounced under high-flow conditions. EC direct estimation via remote sensing remains limited in some studies. (Kaya et al. 2022; Racetin et al. 2020) (Kaya et al. 2022; Racetin et al. 2020) have indirectly assessed EC using salinity as a proxy. A study by Jie Li et al. (2023) that used Sentinel-2 to assess soil salinity in the Yellow River Delta of China found that the SWIR bands are more sensitive to soil salinity. These results are similar to our study's EC estimation in the SWIR bands.

Our study also suggests a potential relationship between EC and suspended solids. Water bodies can contain various inorganic suspended solid matter, such as gravel, sand, silt and clay, which can absorb ions (Zezulka et al. 2024). Moreover, ions have an electrical charge, allowing the water to conduct electricity; therefore, if water has low ions (ions being absorbed), this can decrease the presence of EC in water (Munonde and Selahle 2024). This relationship is supported by the observation that suspended solids – estimated using near-infrared bands (Saberioon et al. 2020) – make bands such as B8 (NIR) to be indirectly sensitive to EC. Under high-flow (wet) conditions, this indicates that RF is robust and capable of revealing non-linear relationships. There are limited studies that focus on using partial dependence plot (PDP) models to predict how non-optically active water quality parameters influence changes or sensitivity in spectral bands, particularly for Sentinel-2. This study aimed to fill this gap by analysing how variations in DO, EC, pH, and temperature influence model predictions of band sensitivity. The PDP results were similar to the PDP contour plot results for all non-optically active water quality parameters. DO refers to the concentration of oxygen gas in water, and its low concentration negatively affects the quality of water needed for aquatic life (Ali and Mishra 2022). Temperature refers to the degree of heat or coldness of water and is influenced by kinetic energy. It varies with season, depth, and, in some cases, time of day (Srivastava et al. 2023). The concentrations and ranges of these two parameters within COHWHS water bodies may also have been influenced by the presence of suspended solids under high-flow conditions. Water with suspended solids retains heat and reduces oxygen levels (Adjovu et al. 2023b).

This is further illustrated in the PDP results, where both DO and temperature were found to influence spectral band sensitivity under high-flow conditions, particularly when DO concentrations were low and temperature ranges were high (and vice versa under low-flow conditions). Furthermore, the PD contour plots illustrate a relationship between DO and temperature, where the temperature needed to be above 27 °C and DO levels between 0 and 6 mg/L for significant band sensitivity. This is supported by Hosna Ara et al. (2017), who highlighted this relationship between the two water quality parameters. In water, pH measures acidity or alkalinity (level = 0–14, with 7 being neutral). This means that levels below 7 indicate acidity, and levels above 7 indicate alkalinity (Yehia and Said 2021). Through the PDP results, our study showed that pH levels between 7 and 8 (under high-flow conditions) contributed to band sensitivity, and these results were similar to those observed under low-flow conditions. This finding indicates that neutral to alkaline pH levels play a role in influencing the band sensitivity. Furthermore, the PDP contour plots revealed that the pH levels needed to exceed 7.5 when combined with other water parameters to affect the band sensitivity. This suggests that neutral to alkaline water in the COHWHS contributes to spectral band sensitivity. In contrast, the relationship between EC and band sensitivity was less straightforward, as no clear difference in concentration was observed between its minimum and maximum values. However, the statistical results (Table 2) showed that EC was slightly lower under high-flow conditions (753.15 μS/cm) compared to low-flow conditions (896 μS/cm). Water is considered slightly saline if the EC ranges between 700 and 2000 μS/cm and moderately saline if the EC ranges between 2000 and 10,000 μS/cm (Rusydi 2018). Based on the mean statistical results from our study, the water bodies within the COHWHS can be considered slightly saline. However, the PDP results indicated that spectral band sensitivity for EC was observed when EC exceeded 1000 μS/cm, suggesting that higher saline concentrations in water lead to greater band sensitivity.

5. Conclusion

This chapter evaluated the sensitivity of Sentinel-2 bands to optically and non-optically active water quality parameters under high-flow and low-flow conditions using three sensitivity analysis models. This study aimed to achieve three key objectives: (1) to determine if significant statistical differences exist in water quality parameters under different flow conditions, (2) to analyze the bivariate relationships between these parameters and Sentinel-2 bands, and (3) to assess the consistency of various sensitivity analysis techniques, MLR, RF variable importance, PDPs with PD contour plots, alongside bivariate correlation analysis in evaluating the sensitivity of spectral bands. This study assessed the sensitivity of Sentinel-2 MSI bands (B1–B8, B8A, B11 and B12) to optically and non-optically active water quality parameters (chlorophyll-*a*, suspended solids, DO, pH, Temperature and EC) under high-flow and low-flow conditions. The statistical results revealed significant differences in water quality parameters between flow conditions. Suspended solids had a stronger influence under high-flow conditions due to increased runoff, whereas chlorophyll-*a* concentrations increased under low-flow conditions when turbidity levels were lower. Non-optically active parameters (DO, pH and EC) were lower under high-flow conditions but increased under low-flow conditions, while Temperature exhibited the opposite trend. Regarding the sensitivity analysis results, bivariate correlation analysis showed a strong positive correlation between the suspended solids and all the Sentinel-2 bands under low-flow conditions. Surprisingly, chlorophyll-*a* correlated strongly with only the coastal aerosol band (B1) under high-flow conditions.

The MLR and RF results confirmed that suspended solids had a stronger influence on spectral band sensitivity than chlorophyll-*a* due to turbidity interference. The study also found that RE bands (B5, B6 and B7) and B3 were not significantly sensitive to chlorophyll-*a*. The PDP results indicated that suspended solids (100–500 mg/L in high-flow, 50–400 mg/L in low-flow) had the greatest influence on the Sentinel-2 band. Chlorophyll-*a* sensitivity was observed at low concentrations (<250 μg/L), except for B6 and B8A, which responded up to 400 μg/L. For non-optically active parameters, DO had a strong negative correlation with most Sentinel-2 bands under both flow conditions, emerging as the primary predictor in the sensitivity analysis, especially in the visible (B2–B4), RE (B5–B7), NIR (B8–B8A) and SWIR (B11–B12) bands. This was attributed to its relationship with suspended solids, chlorophyll-*a* and temperature, which caused DO to have a strong inverse relationship with the spectral bands. pH showed strong positive correlations with the visible and NIR bands, particularly with chlorophyll-*a*. EC had the second strongest influence under low-flow conditions, particularly in SWIR and NIR bands, due to its relationship with suspended solids and salinity. Temperature showed weak spectral sensitivity and was not a strong predictor. PDPs and PD contour plots highlighted key relationships in high-flow conditions where temperatures above 27 °C combined with low DO (0–6 mg/L) led to significant spectral band sensitivity, emphasizing the inverse relationship between temperature and DO. Under low-flow conditions, the spectral sensitivity increased at lower temperatures with higher DO and EC levels. pH exhibited consistent spectral response patterns across both flow conditions.

This study found that the Sentinel-2 RE bands showed low sensitivity to chlorophyll-*a* due to turbidity from suspended solids. Future research should explore spectral indices such as the normalized difference chlorophyll index (NDCI) or the normalized difference vegetation index (NDVI) and consider seasonal variations to improve chlorophyll-*a* detection. Another limitation was that the small sample size (40) collected for this study may have constrained model accuracy, spatial coverage, and sampling frequency, suggesting that future studies should collect more data for better model training, testing, and validation. Additionally, data collection between 9:00 and 15:00 may have introduced biases, as increasing temperatures could have influenced parameter interactions. Moreover, temperature estimation was the least accurate because the Sentinel-2 lacking thermal sensors, emphasizing the need for future research to integrate optical and thermal sensors to enhance the temperature results. To improve the reliability of sensitivity analysis, future studies should explore various GSA approaches to determine the most effective methods. Despite these limitations, the study successfully demonstrated the sensitivity of Sentinel-2 data to both optically and non-optically active water quality parameters, revealing how flow conditions influence these sensitivities. The integration of statistical, bivariate correlation, and sensitivity analysis models highlighted the advantages of combining multiple techniques, contributing to the advancement of remote sensing for water quality monitoring and environmental management.

Author contributions

CRediT: **Sinesipho Ngamile:** Conceptualization, Formal analysis, Investigation, Methodology, Writing – original draft; **Mahlatse Kganyago:** Funding acquisition, Project administration, Resources, Supervision, Writing – review & editing; **Sabelo Madonsela:** Project administration, Supervision, Writing – review & editing; **Vuyelwa Mvandaba:** Data curation.

Disclosure statement

No potential conflict of interest was reported by the author(s).

Funding

The author(s) declare that financial support was received for the research, authorship, and/or publication of this article. This work was supported by the Water Research Commission (WRC) project: Monitoring Surface Water Quality Using Remote Sensing Technology (project number: C2023/2024-01241).

Data availability

The datasets supporting the findings of this study are publicly available in Zenodo at https://doi.org/10.5281/zenodo.17669720 (Ngamile et al., 2025).

References

Abdelmalik KW. 2018. Role of statistical remote sensing for inland water quality parameters prediction. Egyptian Journal of Remote Sensing and Space Science. 21(2):193–200. https://doi.org/10.1016/j.ejrs.2016.12.002

Adjovu GE, Stephen H, James D, Ahmad S. 2023a. Overview of the application of remote sensing in effective monitoring of water quality parameters. Remote Sensing. 15(7):1938. https://doi.org/10.3390/rs15071938

Adjovu GE, Stephen H, James D, Ahmad S. 2023b. Measurement of total dissolved solids and total suspended solids in water systems: a review of the issues, conventional, and remote sensing techniques. Remote Sensing. 15(14):3534. https://doi.org/10.3390/rs15143534

Ahmed M, Mumtaz R, Anwar Z, Shaukat A, Arif O, Shafait F. 2022. A Multi–Step approach for optically active and inactive water quality parameter estimation using deep learning and remote sensing. Water (Switzerland). 14(13):2112. https://doi.org/10.3390/w14132112

Ahmed T, Zounemat-Kermani M, Scholz M. 2020. Climate change, water quality and water-related challenges: a review with focus on Pakistan. International Journal of Environmental Research and Public Health. 17(22):1–22. https://doi.org/10.3390/ijerph17228518

Ali B, Mishra A. 2022. Effects of dissolved oxygen concentration on freshwater fish: a review. International Journal of Fisheries and Aquatic Studies. 10(4):113–127. https://doi.org/10.22271/fish.2022.v10.i4b.2693. A.

Amran MA, Daming WS. 2023. ESTIMATION OF COASTAL WATERS TURBIDITY USING SENTINEL-2 IMAGERY. Geodesy and Cartography (Vilnius). 49(4):180–185. https://doi.org/10.3846/gac.2023.18132
Anghileri D et al. 2024. Global water challenges in sub-saharan Africa and how to strengthen science-policy dialogues on transboundary governance and cooperation. Journal of Environmental Management. 365:121417. https://doi.org/10.1016/j.jenvman.2024.121417
Arora M, Mudaliar A, Pateriya B. 2022. 'Assessment and monitoring of optically active water quality parameters on wetland ecosystems based on remote sensing approach: a case study on harike and keshopur wetland over punjab region, India'. Engineering Proceedings. 27(1):1–9.
Beal MRW, Özdoğan M, Block PJ. 2024. A machine learning and remote sensing-based model for algae pigment and dissolved oxygen retrieval on a small inland lake. Water Resources Research. 60(3):1–18. https://doi.org/10.1029/2023WR035744
Biswas AK, Tortajada C. 2019. Water quality management: a globally neglected issue. International Journal of Water Resources Development. 35(6):913–916. https://doi.org/10.1080/07900627.2019.1670506
Bonneu F, Makowski D, Joly J, Allard D. 2024. Machine learning based on functional principal component analysis to quantify the effects of the main drivers of wheat yields. European Journal of Agronomy. 159:127254. https://doi.org/10.1016/j.eja.2024.127254
Boonprong S, Cao C, Chen W, Bao S. 2018. Random forest variable importance spectral indices scheme for burnt forest recovery monitoring-multilevel RF-VIMP. Remote Sensing. 10(6):807. https://doi.org/10.3390/rs10060807
Bramich J, Bolch CJS, Fischer A. 2021. Improved red-edge chlorophyll-a detection for sentinel 2. Ecological Indicators. 120:106876. https://doi.org/10.1016/j.ecolind.2020.106876
Bresciani M et al. 2019. Monitoring water quality in two dammed reservoirs from multispectral satellite data. European Journal of Remote Sensing. 52(sup4):113–122. https://doi.org/10.1080/22797254.2019.1686956
Brown HKM, Rubega M, Dierssen HM. 2021. The light's in my eyes: optical modeling demonstrates wind is more important than sea surface-reflected sunlight for foraging herons. PeerJ. 9:e12006. https://doi.org/10.7717/peerj.12006
Caballero I, Steinmetz F, Navarro G. 2018. Evaluation of the first year of operational Sentinel-2A data for retrieval of suspended solids in medium- to high-turbiditywaters. Remote Sensing. 10(7):982. https://doi.org/10.3390/rs10070982
Cao Y-N, Li X-H, Ma S-D, Ai J-Y, Zhu H-X. 2018. Urban Water Absorbance to Predict Chlorophyll a and Turbidity. 174:1–8.
Cheng C, Wei Y, Lv G, Yuan Z. 2013. Remote estimation of chlorophyll-a concentration in turbid water using a spectral index: a case study in taihu lake, China. Journal of Applied Remote Sensing. 7(1):073465. https://doi.org/10.1117/1.JRS.7.073465
DeLuca NM, Zaitchik BF, Curriero FC. 2018. Can multispectral information improve remotely sensed estimates of total suspended solids? A statistical study in chesapeake bay. Remote Sensing. 10(9):1393. https://doi.org/10.3390/rs10091393
Deniz V. 2020. Application of multiple linear regression (MLR) analysis for concentration of chromite tailings by the flotation. Physicochemical Problems of Mineral Processing. 56(4):579–589. https://doi.org/10.37190/ppmp/122710
Díaz I et al. 2023. 'Sensitivity analysis for causality in observational studies for regulatory science'. Journal of Clinical and Translational Science. 7(1):1–27.
Durand JF, Meeuvis J, Fourie M. 2010. The threat of mine effluent to the UNESCO status of the Cradle of Humankind World Heritage Site. 6(1). https://doi.org/10.4102/td.v6i1.125
Fanela MAP, Takarina NDSupriatna. 2019. 'Distribution of total suspended solids (TSS) and chlorophyll-a in kendari bay, southeast sulawesi'. In: Journal of Physics: Conference Series. Institute of Physics Publishing.
Fendereski F, Creed IF, Trick CG. 2024a. 'Remote sensing of Chlorophyll-A. in Clear vs. Turbid Waters in Lakes'. 16(19):1–19. https://doi.org/10.3390/rs16193553
Fendereski F, Creed IF, Trick CG. 2024b. Remote sensing of Chlorophyll-a in clear vs. Turbid waters in lakes', *remote sensing*, vol. 16, no. 19. Remote Sensing. 16(19):3553. https://doi.org/10.3390/rs16193553
Gao L, Shangguan Y, Sun Z, Shen Q, Shi Z. 2024. 'Estimation of non-optically active water quality parameters in zhejiang province based on machine learning. Remote Sensing. 16(3):1–19.
Guo J et al. 2024. Investigation of the causes and mechanisms of hypoxia in the central bohai sea in the summer of 2022. Marine Pollution Bulletin. 206:116710. https://doi.org/10.1016/j.marpolbul.2024.116710
Guo J, Wang X, Liu B, Liu K, Zhang Y, Wang C. 2023. 'Remote-Sensing extraction of small water bodies on the loess plateau'. Water. 15(5). Switzerland.
Hasan N, Pushpalatha R, Manivasagam VS, Arlikatti S, Cibin R. 2023. Global sustainable water management: a systematic qualitative review. Water Resources Management. 37(13):5255–5272. https://doi.org/10.1007/s11269-023-03604-y
Hobbs PJ. 2017. TDS load contribution from acid mine drainage to hartbeespoort dam, South Africa. Water SA. 43(4):626–637. https://doi.org/10.4314/wsa.v43i4.10
HosnaAra M, Nazim Uddin U, Chandra Sarkar S, Kumar U. 2017. 'Seasonal variation of temperature dependent physico-chemical parameters of a coastal river bhadra, Bangladesh'. Journal of Tropical Biology and Conservation. 14:69–81.

Hutchings AM, de Vries CS, Hayes NR, Orr HG. 2024. Temperature and dissolved oxygen trends in English estuaries over the past 30 years. Estuarine, Coastal and Shelf Science. 306:108892. https://doi.org/10.1016/j.ecss.2024.108892

Jang W et al. 2024. Evaluation of Sentinel-2 based Chlorophyll-a estimation in a small-scale reservoir: assessing accuracy and availability. Remote Sensing. 16(2):315. https://doi.org/10.3390/rs16020315

Jaywant SA, Arif KM. 2024. Remote sensing techniques for water quality monitoring: a review. Sensors. 24(24):8041. https://doi.org/10.3390/s24248041

Jiang D et al. 2023. Estimating the concentration of total suspended solids in inland and coastal waters from Sentinel-2 MSI: a semi-analytical approach. ISPRS Journal of Photogrammetry and Remote Sensing. 204:362–377. https://doi.org/10.1016/j.isprsjprs.2023.09.020

Johnson PM, Barbour W, Camp JV, Baroud H. 2022. Using machine learning to examine freight network spatial vulnerabilities to disasters: a new take on partial dependence plots. Transportation Research Interdisciplinary Perspectives. 14:100617. https://doi.org/10.1016/j.trip.2022.100617

Joshi JK et al. 2025. Empirical modelling of suspended sediments using spectral data from spectroradiometer and sentinel-2 in mula dam reservoir, maharashtra, India. Scientific Reports. 15(1):34205. https://doi.org/10.1038/s41598-025-15719-w

Kaya F, Schillaci C, Keshavarzi A, Başayiğit L. 2022. Predictive mapping of electrical conductivity and assessment of soil salinity in a Western Türkiye alluvial plain. Land. 11(12):2148.

Kim SW, Jung D, Choung YJ. 2020. Development of a multiple linear regression model for meteorological drought index estimation based on landsat satellite imagery. Water (Switzerland). 12(12):3393. https://doi.org/10.3390/w12123393

Lavanya C, Nikitha M, Swetha N, Nikhitha K, Hussein L. 2024. Assessment and estimation of water quality using multi-linear regression', in. E3S Web of Conferences. 529:03007. https://doi.org/10.1051/e3sconf/202452903007. EDP Sciences.

Li J et al. 2022. 'Satellite detection of surface water extent: a review of methodology'. Water. 14(7). Switzerland.

Li J, Zhang T, Shao Y, Ju Z. 2023. 'Comparing machine learning algorithms for soil salinity mapping using topographic factors and Sentinel-1/2 data: a case study in the Yellow River delta of China'. Remote Sensing. 15(9).

Li L et al. 2023. An advanced remote sensing retrieval method for urban non-optically active water quality parameters: an example from shanghai. Science of the Total Environment. 880:1–12. https://doi.org/10.1016/j.scitotenv.2023.163389

Liu H, Li Q, Shi T, Hu S, Wu G, Zhou Q. 2017. Application of sentinel 2 MSI images to retrieve suspended particulate matter concentrations in poyang lake. Remote Sensing. 9(7):761. https://doi.org/10.3390/rs9070761

Liu M, Wang L, Qiu F. 2022. Using MODIS data to track the long-term variations of dissolved oxygen in lake taihu. Frontiers in Environmental Science. 10. https://doi.org/10.3389/fenvs.2022.1096843

Liu Y, Zhao H. 2017. Variable importance-weighted random forests. Quantitative Biology. 5(4):338–351. https://doi.org/10.1007/s40484-017-0121-6

Llodrà-Llabrés J, Martínez-López J, Postma T, Pérez-Martínez C, Alcaraz-Segura D. 2023. Retrieving water chlorophyll-a concentration in inland waters from Sentinel-2 imagery: review of operability, performance and ways forward. International Journal of Applied Earth Observation and Geoinformation. 125:103605.

Loaiza JG et al. 2023a. Surface water quality assessment through remote sensing based on the Box–Cox transformation and linear regression. Water (Switzerland). 15(14).

Loaiza JG et al. 2023b. Surface water quality assessment through remote sensing based on the Box–Cox transformation and linear regression. Water (Switzerland). 15(14).

Lolli S, Alparone L, Arienzo A, Garzelli A. 2024. Characterizing dust and biomass burning events from Sentinel-2 imagery. Atmosphere. 15(6):672. https://doi.org/10.3390/atmos15060672

Ly HB, Nguyen TA, Pham BT. 2022. Investigation on factors affecting early strength of high-performance concrete by Gaussian process regression. PLoS ONE. 17(1):e0262930. https://doi.org/10.1371/journal.pone.0262930.

Makanda K, Nzama S, Kanyerere T. 2022. Assessing the role of water resources protection practice for sustainable water resources management: a review. Water (Switzerland). 14(19):3153. https://doi.org/10.3390/w14193153

McCarthy TS. 2011. The impact of acid mine drainage in South Africa. South African Journal of Science. 107(5/6):7 pages. https://doi.org/10.4102/sajs.v107i5/6.712

Mpakairi KS, Dube T, Sibanda M, Mutanga O. 2023. Fine-scale characterization of irrigated and rainfed croplands at national scale using multi-source data, random forest, and deep learning algorithms. ISPRS Journal of Photogrammetry and Remote Sensing. 204:117–130. https://doi.org/10.1016/j.isprsjprs.2023.09.006

Mpakairi KS, Muthivhi FF, Dondofema F, Munyai LF, Dalu T. 2024. Chlorophyll-a unveiled: unlocking reservoir insights through remote sensing in a subtropical reservoir. Environmental Monitoring and Assessment. 196(4):401. https://doi.org/10.1007/s10661-024-12554-w

Munonde TS, Selahle SK. 2024. Comparative seasonal trends and potential health impacts of arsenic and chromium in surface water after adsorption using highly dispersed Fe3O4 nanoparticles. Analytical Science Advances. 5:1–15. https://doi.org/10.1002/ansa.202400045

Nasseri S, Farhadi Bansouleh B, Azari A. 2023. Estimation of land surface temperature in agricultural lands using sentinel 2 images: a case study for sunflower fields. Irrigation and Drainage. 72(3):796–806. https://doi.org/10.1002/ird.2802

Ndou N. 2023. Geostatistical inference of Sentinel-2 spectral reflectance patterns to water quality indicators in the setumo dam, South Africa. Remote Sensing Applications: Society and Environment. 30:100945. https://doi.org/10.1016/j.rsase.2023.100945

Ngamile Sinesipho, Kganyago Mahlatse, Madonsela Sabelo, Mvandaba Vuyelwa. 2025. Characterising the spatio-temporal patterns of water quality parameters in the cradle of humankind world heritage site using Sentinel-2 and random forest regressor. Frontiers in Remote Sensing. 6. https://doi.org/10.3389/frsen.2025.1631403

Ottaviani M et al. 2008. Light reflection from water waves: suitable setup for a polarimetric investigation under controlled laboratory conditions. Journal of Atmospheric and Oceanic Technology. 25(5):715–728. https://doi.org/10.1175/2007JTECHA1049.1

Oyem HH, Oyem IM, Ezeweali D. 2014. Temperature, pH, electrical conductivity, total dissolved solids and chemical oxygen demand of groundwater in Boji-BojiAgbor/Owa area and immediate suburbs. Research Journal of Environmental Sciences. 8(8):444–450. https://doi.org/10.3923/rjes.2014.444.450

Parsania MrPS, Virparia DV. 2016. A comparative analysis of image interpolation algorithms. IJARCCE. 5(1):29–34. https://doi.org/10.17148/IJARCCE.2016.5107

Pasaribu RA, Budi PS, Saharani AA, Hutagalung DG, Ramadhan R. 2024. Temporal detection of total suspended solid (TSS) distribution in the Southern area of obi island', in. BIO Web of Conferences. 106:04012. https://doi.org/10.1051/bioconf/202410604012

Poursanidis D, Traganos D, Reinartz P, Chrysoulakis N. 2019. On the use of Sentinel-2 for coastal habitat mapping and satellite-derived bathymetry estimation using downscaled coastal aerosol band. International Journal of Applied Earth Observation and Geoinformation. 80:58–70. https://doi.org/10.1016/j.jag.2019.03.012

Racetin I, Krtalic A, Srzic V, Zovko M. 2020. Characterization of short-term salinity fluctuations in the neretva river delta situated in the Southern adriatic Croatia using Landsat-5 TM. Ecological Indicators. 110:105924. https://doi.org/10.1016/j.ecolind.2019.105924

Razavi S, Gupta HV. 2015. What do we mean by sensitivity analysis? The need for comprehensive characterization of "global" sensitivity in earth and environmental systems models. Water Resources Research. 51(5):3070–3092. https://doi.org/10.1002/2014WR016527

Razavi S et al. 2021. The future of sensitivity analysis: an essential discipline for systems modeling and policy support. Environmental Modelling and Software. 137:104954. https://doi.org/10.1016/j.envsoft.2020.104954

Rodriguez-Galiano VF, Ghimire B, Rogan J, Chica-Olmo M, Rigol-Sanchez JP. 2012. An assessment of the effectiveness of a random forest classifier for land-cover classification. ISPRS Journal of Photogrammetry and Remote Sensing. 67(1):93–104. https://doi.org/10.1016/j.isprsjprs.2011.11.002

Rusydi AF. 2018. 'Correlation between conductivity and total dissolved solid in various type of water: a review'. In: IOP Conference Series: Earth and Environmental Science. 118. Institute of Physics Publishing. 012019. https://doi.org/10.1088/1755-1315/118/1/012019

Saberioon M, Brom J, Nedbal V, Souček P, Císař P. 2020. Chlorophyll-a and total suspended solids retrieval and mapping using Sentinel-2A and machine learning for inland waters. Ecological Indicators. 113:106236. https://doi.org/10.1016/j.ecolind.2020.106236

Sagan V et al. 2020. 'Monitoring inland water quality using remote sensing: potential and limitations of spectral indices, bio-optical simulations, machine learning, and cloud computing'., Earth-Science Reviews. 205:103187. https://doi.org/10.1016/j.earscirev.2020.103187

Salas EAL, Kumaran SS, Partee EB, Willis LP, Mitchell K. 2022. Potential of mapping dissolved oxygen in the Little Miami River using Sentinel-2 images and machine learning algorithms. Remote Sensing Applications: Society and Environment. 26:1–14.

Saltelli A, Puy A, Lo Piano S. 2021. 'Sensitivity analysis. SSRN Electronic Journal. 1–10. Available from: https://www.ssrn.com/abstract=3977108

Savoy P, Harvey JW. 2023. Predicting daily river chlorophyll concentrations at a continental scale. Water Resources Research. 59(11):1–16. https://doi.org/10.1029/2022WR034215

Sent G et al. 2021. Deriving water quality parameters using sentinel-2 imagery: a case study in the sado estuary, Portugal. Remote Sensing. 13(5):1–30. https://doi.org/10.3390/rs13051043

Sfravara F, Barberi E, Bongiovanni G, Chillemi M, Brusca S. 2024. Development of a predictive model for evaluation of the influence of various parameters on the performance of an oscillating water column device. Sensors. 24(11):3582. https://doi.org/10.3390/s24113582

Shafiullah AZ, Werner J, Kennedy E, Leso L, O'brien B, Umstätter C. 2019. Machine learning based prediction of insufficient herbage allowance with automated feeding behaviour and activity data. Sensors (Switzerland). 19(20):4479. https://doi.org/10.3390/s19204479

Soomets T, Uudeberg K, Jakovels D, Brauns A, Zagars M, Kutser T. 2020. Validation and comparison of water quality products in baltic lakes using sentinel-2 msi and sentinel-3 OLCI data. Sensors (Switzerland). 20(3):742. https://doi.org/10.3390/s20030742

Srivastava MK, Gaur S, Ohri A, Srivastava PK, Singh N. 2023. 'Applications of remote sensing in water quality assessment', in. Remote Sensing in Precision Agriculture: Transforming Scientific Advancement into Innovation. Elsevier; p. 217–236.

Tami M et al. 2018. Uncertain Trees: Dealing with Uncertain Inputs in Regression Trees. 1–9. Available from: http://arxiv.org/abs/1810.11698
Thakur A, Devi P. 2024. A comprehensive review on water quality monitoring devices: materials advances, current status, and future perspective. Critical Reviews in Analytical Chemistry. 54(2):193–218. https://doi.org/10.1080/10408347.2022.2070838
Usali N, Ismail H. 2010. Use of remote sensing and GIS in monitoring water quality. Journal of Sustainable Development. 3(3):p228. https://doi.org/10.5539/jsd.v3n3p228
Viso-Vázquez M, Acuña-Alonso C, Rodríguez JL, Álvarez X. 2021. Remote detection of cyanobacterial blooms and chlorophyll-a analysis in a eutrophic reservoir using sentinel-2. In: Sustainability. 13(15). Switzerland.
Windisch J et al. 2022. Toxic elements in sediment and water of the crocodile river (West) system, South Africa, following acid mine drainage. Applied Sciences (Switzerland). 12(20):10531. https://doi.org/10.3390/app122010531
Wolters Erwin, Toté Carolien, Sterckx Sindy, Adriaensen Stefan, Henocq Claire, Bruniquel Jérôme, Scifoni Silvia, Dransfeld Steffen. 2021. iCOR Atmospheric Correction on Sentinel-3/OLCI over Land: Intercomparison with AERONET, RadCalNet, and SYN Level-2. Remote Sensing. 13:654654. https://doi.org/10.3390/rs13040654
Wu Z et al. 2018. Interactions between water vapor and atmospheric aerosols have key roles in air quality and climate change. National Science Review. 5(4):452–454. https://doi.org/10.1093/nsr/nwy063
Xiao Y et al. 2023. Monitoring of chlorophyll-a and suspended sediment concentrations in optically complex inland rivers using multisource remote sensing measurements. Ecological Indicators. 155:111041. https://doi.org/10.1016/j.ecolind.2023.111041
Xin-hui W, Cai-lan G, Yong H, Lan L, Zhi-jie H. 2021. 'Spectral feature construction and sensitivity analysis of water quality parameters remote sensing inversion'. Spectroscopy and spectral analysis. 41(06):1–9.
Yang Q. 2017. Regression. In: Encyclopedia of Big Data. Springer International Publishing: Cham. p 1–4. https://doi.org/10.1007/978-3-319-32001-4_174-1
Yehia HMA-S, Said SM. 2021. Drinking water treatment: pH adjustment using natural physical field. Journal of Biosciences and Medicines. 09(06):55–66. https://doi.org/10.4236/jbm.2021.96005
Yin F, Yang G, Yan M, Xie Q. 2019. Application of multispectral remote sensing technology in water quality monitoring. Desalination and Water Treatment. 149:363–369. https://doi.org/10.5004/dwt.2019.23857
Zainurin SN et al. 2022. Advancements in monitoring water quality based on various sensing methods: a systematic review. International Journal of Environmental Research and Public Health. 19(21):14080. https://doi.org/10.3390/ijerph192114080
Zezulka Š, Maršálek B, Maršálková E, Odehnalová K, Pavlíková M, Lamaczová A. 2024. Suspended particles in water and energetically sustainable solutions of their Removal—A review. Processes. 12(12):2627. https://doi.org/10.3390/pr12122627
Zhang XY, Trame MN, Lesko LJ, Schmidt S. 2015. Sobol sensitivity analysis: A tool to guide the development and evaluation of systems pharmacology models. CPT: Pharmacometrics and Systems Pharmacology. 4(2):69–79.
Zhang Y, Wu F, Wong KP, Feng J, Chang J, Qiu J. 2026. 'Remote sensing retrieval of Chlorophyll-a in turbid waters using Sentinel-3 OLCI: application of machine learning in the pearl river estuary (China). Journal of Marine Science and Engineering. 14(4):1–18.